Dynamical Gravity, Expanding Space and Stretching Gedesics

Clive Anthony Redwood (caredwood@outlook.com)
Independent Researcher https://orcid.org/0000-0002-5494-7924

Research Article

Keywords: gravitation, Hubble expansion, dark energy, dark matter

Posted Date: June 3rd, 2021

DOI: https://doi.org/10.21203/rs.3.rs-577905/v1

Dynamical Gravity, Expanding Space and Stretching Geodesics

Clive A. Redwood[1]

Abstract

The gravitational natures of phenomena separately attributed to dark matter and dark energy and challenges encountered in identifying such sources motivate enquiry into the capabilities of the field, itself, to generate such phenomena. It is found that, in curvature-free Friedmann-Lemaître-Robertson-Walker and gravitationally perturbed Robertson-Walker spacetimes, gravity has an equation of state parameter $w = -1$ and negative pressures. Expanding space is proposed as the form of a growing cosmic gravitational field. The gravitational-spatial expansion is locally isobaric. Barotropic gravitational dynamics yield the Hubble-Lemaître law. The expansion results from the induction of gravity by matter, radiation and by itself. Gravitational auto-induction is a dynamical feedback process that produces an isotropic spatial expansion with an invariant Hubble parameter like a 'cosmological constant' of density $2H^2/\kappa$ or, equivalently, of a density parameter of $2/3$. The *Planck* 2018 result is moderately higher at about the 2.5σ level. A new expression of the Hubble parameter in the late homogeneous universe is obtained. The growth of the field isotropically stretches geodesics. In homogeneous regions, this manifests as the Hubble acceleration of bodies and the redshifting of radiation attributed to dark energy. Geodesics may depend on gravitational energy density that retains its values at comoving locations. In inhomogeneous regions, such retentions lead to similar retentions of circular speeds and deflection angles - geodesic stretching - attributed to clustering dark matter. The baryonic Tully-Fisher relation is explained. Dependence of geodesics on gravitational energy explains tidal interactions as being inertial gravitational processes.

Key words: gravitation, Hubble expansion, dark energy, dark matter

1.0 Introduction

In an effort to obtain a finite static universe, Einstein proposed a cosmological constant in an additive term in his general field equations. [1] On the empirical establishment of the Hubble expansion, he withdrew this proposal. Clearly, Einstein expected that the universe's expansion could be explained without recourse to a cosmological constant. This may imply an inherent instability in Einstein's field equations. The source of such a spacetime instability may be the source of both the spatial expansion and the extended geodesics.

An examination of Einstein's derivation of the field equations [2] has revealed an underlying gravitational process that is inherently unstable. Presented, here, is an exploration of this dynamical process with regards to its potential to explain the large-scale expansion and the extension of the small-scale geodesics.

These considerations arise in the absence of a widely accepted theory that explains the apparently mutually exclusive sets of dynamic phenomena separately attributed to hypothesized dark energy (DE) and dark matter (DM). So, there occurs a dichotomy within gravitational science. The Friedmann-Lemaître-Robertson-Walker (FLRW) theory of an expanding universe without spatial curvature at large scales, with its determinations of the spatial expansion, continues to be affirmed by observations. However, at relatively small scales - such as in solar systems, galaxies, superclusters, that is, for gravitationally bound systems - it is not applicable.

[1] Clive A. Redwood
ORCHID: 0000-0002-5494-7924
Independent Researcher
14 June Road, Kingston 7, Jamaica, W.I.
caredwood@outlook.com,
Tel.: +1-876-576-8763

Theoretical explorations of the relations of spacetimes applicable to galaxies, on one hand and, on the other, to very large, effectively homogeneous, regions have not changed this situation. In fact, in 1945, Einstein and Straus, in [3], established the conditions for the coexistence of the spherically symmetric static Schwarzschild spacetime - that explained significant phenomena at the scale of our solar system - and the FLRW spacetime. However, the two had to be mutually excluded in space and they only had external relations, with the small-scale Schwarzschild spacetimes simply existing in spherical *vacuoles* [4,5] transported in the Hubble flow within the FLRW spacetime. It has been shown that such coexistence is fragile for the Schwarzschild spacetime, with instability under isotropic radial changes and vulnerability to non-spherical perturbations [4]. This Einstein-Straus 'Swiss cheese' model has remained, in theory, the fundamental architecture of the cosmos. [4]

Nevertheless, there have been attempts to develop unitary explanations of gravitational phenomena separately ascribed to DM and DE. These include [6] that proposes the coexistence of bodies with negative and positive masses in a modified ΛCDM universe and [7] that proposes, in a modification of Friedmann's theory, that gravity acts, across all scales, in the manner of the strong force of quantum chromodynamics.

The endeavour, here, is to develop a unitary explanation - completely within the paradigm of Einstein's gravitational field theory [2] - that explains both sets of phenomena. The intent is to include the universal empirical element of the Hubble expansion of space [8] without resort to exotic agencies.

A barotropic nature of gravitational fields in spatially flat and expanding spacetimes is established and ensuing dynamics explored in §2. In §3 and §4, gravitational induction is explored and its potential relations with the spatial expansion are developed. Effects of the expansion on geodesics are explored and relations between gravitational energy density and geodesics are developed in §5. Certain tidal interactions of the gravitational fields variously associated with stellar systems are explored in §6. In §7, there is a discussion of aspects of the views presented here. Conclusions of the explanations given here and the direction of future work are summarized in §8.

2.0 Barotropic gravity

2.1 A generalized FLRW spacetime

It is clear that the spatial homogeneity is only approximated at very large scales in the universe. So, in order to accommodate small-scale phenomena [9], the principle of homogeneity has to be surrendered.

However, the universe still appears fairly isotropic [10] as observed from within our solar system and since galaxies display galactocentric kinematics and distributions of matter, then a spherically symmetric metric seems appropriate. Most important in the choice of a spacetime is the fact that the cosmic expansion is isotropic and its fundamental relation, the Hubble-Lemaître law, is linear.

Consider a universe with a spherically symmetric line element of the form:

$$(\mathrm{d}s)^2 = g_{tt}(\mathrm{d}x^0)^2 + g_{rr}\,[(\mathrm{d}x^1)^2 + (\mathrm{dx}^2)^2 + (\mathrm{d}x^3)^2] \tag{1}$$

Now, in observance of the empirically supported universal isotropy, rewrite as:

$$(\mathrm{d}s)^2 = g_{tt}(\mathrm{d}x^t)^2 + g_{rr}(\mathrm{d}x^r)^2 \tag{2}$$

Where:

$$\mathrm{d}x^r = \mathrm{d}r = [(\mathrm{d}x^1)^2 + (\mathrm{dx}^2)^2 + (\mathrm{d}x^3)^2]^{1/2} \tag{3}$$

The line element - $\mathrm{d}s$ - is the invariant locally determined distance, or duration, corresponding to the infinitesimal coordinate vector components $\mathrm{d}x^{\nu}$ by means of the $g_{\mu\nu}$ that are components of the metric, with tensorial indices $\mu, \nu = 0, 1, 2, 3$. Equation (1), that permits a curvilinear g_{tt} and a g_{rr} that may also depend on location, generalizes the spatially flat FLRW equation of the linear element, with a time positive signature, that has $g_{tt} = 1$ and $g_{rr} = -a^2$, where $a = a(x^t)$ is the dimensionless time-dependent scale factor, $x^t = \mathrm{c}t$, c is the maximum speed of light, and t is time in seconds.

Equation (2) specifies the line element in an isotropic coordinate frame that simplifies descriptions in the isotropic applications that ensue.

2.2 A Gravitational barotrope

The gravitational field components are, here, defined by the negative of the Christoffel symbol of the second kind:

$$\Gamma^{\tau}_{\mu\nu} = -\frac{g^{\sigma\tau}}{2}\left(\frac{\partial g_{\mu\sigma}}{\partial x^{\nu}} + \frac{\partial g_{\nu\sigma}}{\partial x^{\mu}} - \frac{\partial g_{\mu\nu}}{\partial x^{\sigma}}\right) \tag{4}$$

Where, $g^{\sigma\tau}$ are components of the inverse metric. (This is the original definition of the gravitational field components given by Einstein [2]. It is the negative of that given, for example, in the influential [11].)

Substitutions of the tensorial Greek indices by those of the isotropic frame beginning with r yields:

$$\Gamma^{\mathrm{r}}_{\mathrm{rr}} = -\frac{g^{rr}}{2}\left(\frac{\partial g_{rr}}{\partial x^{r}} + \frac{\partial g_{rr}}{\partial x^{r}} - \frac{\partial g_{rr}}{\partial x^{r}}\right) = -\frac{g^{rr}}{2}\frac{\partial g_{rr}}{\partial x^{r}} \tag{5}$$

Similarly obtained, the other field components are:

$$\Gamma^{\mathrm{t}}_{\mathrm{tt}} = -\frac{g^{tt}}{2}\frac{\partial g_{tt}}{\partial x^{t}} \tag{6}$$

$$\Gamma^{\mathrm{r}}_{\mathrm{rt}} = \Gamma^{\mathrm{r}}_{\mathrm{tr}} = -\frac{g^{rr}}{2}\frac{\partial g_{rr}}{\partial x^{t}} \tag{7}$$

$$\Gamma^{\mathrm{t}}_{\mathrm{rt}} = \Gamma^{\mathrm{t}}_{\mathrm{tr}} = -\frac{g^{tt}}{2}\frac{\partial g_{tt}}{\partial x^{r}} \tag{8}$$

$$\Gamma^{\mathrm{r}}_{\mathrm{tt}} = \frac{g^{rr}}{2}\frac{\partial g_{tt}}{\partial x^{r}} \tag{9}$$

$$\Gamma^{\mathrm{t}}_{\mathrm{rr}} = \frac{g^{tt}}{2}\frac{\partial g_{rr}}{\partial x^{t}} \tag{10}$$

Within the coordinate constraint $\sqrt{-g} = 1$ where g is the determinant of the metric, the energetic flux densities of gravity are given in [2] as the pseudo-tensors:

$$\hat{t}^{\alpha}_{\sigma} = \frac{1}{\kappa}\left(\frac{\delta^{\alpha}_{\sigma}}{2} g^{\mu\nu}\Gamma^{\lambda}_{\mu\beta}\Gamma^{\beta}_{\nu\lambda} - g^{\mu\nu}\Gamma^{\alpha}_{\mu\beta}\Gamma^{\beta}_{\nu\sigma}\right) \tag{11}$$

Where, $\kappa = 8\pi \mathrm{G}/\mathrm{c}^2$ is the Einstein constant, G is Newton's constant, and δ^{α}_{σ} is the Kronecker delta.

The expansion of space has usefully been ascribed to barotropic agents. These include DE [8], for example, and the false vacuum of inflation [12]. So, here, the gravitational field will be examined to determine its suitability for such a role.

Now, only the diagonal elements of the gravitational energy pseudo-tensors $\hat{t}^{\alpha}_{\alpha}$ (or energy tensors) are associated with changes of volume. These elements are normal stresses and energy density. Momentum flux densities and transverse energetic fluxes, such as shear stresses, do not change volumes. So, at first, setting the indexes α and σ to r in eq. (11) and applying the Einstein summation rule yields:

$$\kappa\hat{t}^{r}_{r} = \frac{g^{rr}}{2}\Gamma^{\lambda}_{r\beta}\Gamma^{\beta}_{r\lambda} - g^{rr}\Gamma^{r}_{r\beta}\Gamma^{\beta}_{rr} + \frac{g^{tt}}{2}\Gamma^{\lambda}_{t\beta}\Gamma^{\beta}_{t\lambda} - g^{tt}\Gamma^{r}_{t\beta}\Gamma^{\beta}_{tr} \tag{12}$$

With further substitutions of tensorial indices and applications of the summation rule, then the above equation becomes:

$$\kappa\hat{t}^{r}_{r} = -\frac{g^{rr}}{2}\Gamma^{\mathrm{r}}_{\mathrm{rr}}\Gamma^{\mathrm{r}}_{\mathrm{rr}} + \frac{g^{rr}}{2}\Gamma^{\mathrm{t}}_{\mathrm{rt}}\Gamma^{\mathrm{t}}_{\mathrm{rt}} - \frac{g^{tt}}{2}\Gamma^{\mathrm{r}}_{\mathrm{rt}}\Gamma^{\mathrm{r}}_{\mathrm{rt}} + \frac{g^{tt}}{2}\Gamma^{\mathrm{t}}_{\mathrm{tt}}\Gamma^{\mathrm{t}}_{\mathrm{tt}} \tag{13}$$

Proceeding similarly, by first setting $\alpha = \sigma = t$ in eq. (11) and so on, as before, or simply by interchanging the indices r and t in the above equation, then the other energetic gravitational flux density of interest here, $\hat{t}^{t}_{t}$, is given in:

$$\kappa\hat{t}^{t}_{t} = \frac{g^{rr}}{2}\Gamma^{\mathrm{r}}_{\mathrm{rr}}\Gamma^{\mathrm{r}}_{\mathrm{rr}} - \frac{g^{rr}}{2}\Gamma^{\mathrm{t}}_{\mathrm{rt}}\Gamma^{\mathrm{t}}_{\mathrm{rt}} + \frac{g^{tt}}{2}\Gamma^{\mathrm{r}}_{\mathrm{rt}}\Gamma^{\mathrm{r}}_{\mathrm{rt}} - \frac{g^{tt}}{2}\Gamma^{\mathrm{t}}_{\mathrm{tt}}\Gamma^{\mathrm{t}}_{\mathrm{tt}} \tag{14}$$

Therefore:

$$\hat{t}_t^t = -\hat{t}_r^r \tag{15}$$

The diagonal elements of the gravitational pseudo-tensors are:

$$\text{diag}\{\hat{t}_\delta^\alpha\} = [\hat{t}_0^0, \hat{t}_1^1, \hat{t}_2^2, \hat{t}_3^3] \tag{16}$$

Where, the first element in the square brackets $\hat{t}_0^0$ is the energy density, here also denoted as $\hat{t}_t^t$. The other elements - $\hat{t}_i^i$ for $i = 1, 2, 3$ - are normal stresses that, within the isotropic gravitational field, are all equal to the gravitational pressure $\hat{t}_r^r$. Therefore, regarding gravity in generalized FLRW spacetimes as a fluid, eq. (15) reveals that it has an equation of state (*EoS*) parameter, the ratio of the pressure to the energy density, of $w = -1$.

The FLRW spacetime is widely acknowledged as one that provides descriptions of the spatial expansion at large scales. Substituting its metric components $g_{rr} = -a^2$ and $g_{tt} = 1$ into the expressions of the field components given in eqs. (5) to (10) results in the vanishing of all the field components with the exceptions of $\Gamma^{\mathrm{t}}_{\mathrm{rr}}$ and $\Gamma^{\mathrm{r}}_{\mathrm{rt}} = -\dot{a}/a = -H$, where H is the Hubble parameter. Substituting the latter field component into (13) yields the gravitational pressure: $\hat{t}_r^r = -(\Gamma^{\mathrm{r}}_{\mathrm{rt}})^2/2\kappa = -H^2/2\kappa < 0$. A similar substitution in eq. (14) yields the gravitational energy density as $\hat{t}_t^t = (\Gamma^{\mathrm{r}}_{\mathrm{rt}})^2/2\kappa = H^2/2\kappa = -\hat{t}_r^r$. So, the gravitational field in the curvature-free FLRW spacetime possesses the significant barotrope characterized by an *EoS* parameter of $w = -1$ and negative pressure.

2.3 The barotropic dynamics of gravity and the spatial expansion

The foregoing naturally motivates consideration of the barotropic dynamics of the gravitational field in relation to the spatial expansion. Such an expansion of space is simplest conceived as resulting from its coincidence with an expanding barotropic gravitational field.

Any expansion of the gravitational field would occur under the constraints of its two energy conservation laws, one in the absences of matter and radiation and the other of the 'total system' - the latter including matter and/or radiation and the gravitational field - expressed, respectively, in [2] as:

$$\frac{\partial \hat{t}_\mu^\sigma}{\partial x^\sigma} = 0 \tag{17}$$

and

$$\frac{\partial}{\partial x^\sigma}(\hat{t}_\mu^\sigma + T_\mu^\sigma) = 0 \tag{18}$$

Where, T_μ^σ is the energy tensor of matter and, or, radiation.

Equation (17) expresses the divergence-free (divergenceless everywhere) nature of the energetic flux densities of gravity. That is, locally, the *densities of energetic gravitational fluxes do not change*.

Expansion of the gravitational field, under this constraint, implies *increasing energy* that only develops in *emergent fields* that come into being in simultaneously *emergent* infinitesimal *spaces* at the same energy densities as that of the infinitesimal regions of the pre-existent gravitational field contiguous to these infinitesimal emergent spaces. So, the expansion of space would occur as a smooth interstitial emergence of the gravitational field in new spaces throughout the pre-existent spatial manifold. This may occur, most simply, if *space is the form of the transparent gravitational field*. This notion is buttressed by the *singular* metric coupling of the gravitational field and space expressed by eqs. (1) and (4).

Now, since the gravitational energy flux densities are conserved, then a gravitationally driven expansion, in an isotropic universe, would be locally isobaric. All isobaric expansions require the injection of energy. In thermodynamics, this is in the form of heat transfer. In the non-thermal isobaric gravitational expansion of space, emergent gravitational energy - that, by virtue of the constraint of the conservation of gravitational energy density, may only occur in emergent spaces – may perform the same role in the expansion of space as heat transfer does in isobaric thermodynamic expansions.

Consider the isobaric expansion of the gravitational field as a spatial expansion of a sphere resulting in an incremental volume in the form of a spherical shell of inner radius r and infinitesimal thickness $\mathrm{d}r$. This expansion is due to the work that is done by the gravitational pressure through the displacement $\mathrm{d}r$ that yields the emergent volume in the form of the shell.

Let $\mathrm{d}W$ be the work done by the gravitational pressure $\hat{t}_r^r$ and $\mathrm{d}U$ be the gravitational energy at a density $\hat{t}_t^t$ emerging in the simultaneously emergent space solely as a result of the gravitational pressure. The work $\mathrm{d}W$ is the product of the pressure, the area of the inner surface of the shell - $4\pi r^2$, and the displacement and is, here, expressed as:

$$\mathrm{d}W = 4\pi r^2 \hat{t}_r^r \mathrm{d}r \tag{19}$$

Recall the volume of the sphere:

$$V = \frac{4}{3}\pi r^3 \tag{20}$$

The isotropic expansion of gravity results in the emergence of space of infinitesimal volume:

$$\mathrm{d}V = 4\pi r^2 \mathrm{d}r \tag{21}$$

In this non-thermal process, conservation of energy, during the expansion, requires that $\mathrm{d}W + \mathrm{d}U = 0$, so:

$$\mathrm{d}U = -\mathrm{d}W = -4\pi r^2 \hat{t}_r^r \mathrm{d}r \tag{22}$$

Then, eqs. (19), (21), (22) and (15) yield the resulting energy density within the shell as:

$$\rho = \frac{\mathrm{d}U}{\mathrm{d}V} = -\frac{4\pi r^2 \hat{t}_r^r \mathrm{d}r}{4\pi r^2 \mathrm{d}r} = -\hat{t}_r^r = \hat{t}_t^t \tag{23}$$

This shows how emergent spaces develop and are simultaneously occupied by incremental gravitational energy at local pre-existent densities through the actions of the gravitational pressure at local pre-existent intensities.

It follows that the gravitational field has no rest energy and, therefore, its perturbations travel at the speed of light. This is consistent with predictions of Einstein's linearized field theory of gravitational waves (GWs) in the far field. This has been strongly supported by GW evidence garnered from the binary neutron star merger and the associated gamma-ray burst (GRB) in events labelled, respectively, as GW170817 and GRB 170817A by the detection of a delay of < 2 s between the arrivals of the gravitational waves and the gamma rays after traveling for more than 100 million years. [13]

Consider the expansion of space as it occurs in two separate spherical regions - each of arbitrary and increasing radius. The spheres are located in gravitational fields, possibly of different gravitational pressures. The objective, firstly, is to compare the rates of fractional volumetric increase of space that result from these pressures.

The power per unit volume, injected isobarically throughout a sphere, is directly proportional to the constant gravitational pressure applied. That is:

$$\frac{1}{V}\frac{\mathrm{d}W}{\mathrm{d}x^{\mathrm{t}}} \propto \hat{t}_r^r$$

In these non-thermal isobaric expansions $dW = \hat{t}_r^r dV$, as eqs. (21) and (22) affirm. So, the power, per unit volume of the sphere, delivered by the pressure is given by:

$$\frac{1}{V}\frac{\mathrm{d}W}{\mathrm{d}x^t} = \frac{\hat{t}_r^r}{V}\frac{\mathrm{d}V}{\mathrm{d}x^t} \tag{25}$$

Denoting the two scenarios of the expanding spheres by the indices 1 and 2, respectively, the two relations above may be combined as:

$$\frac{\hat{t}^r_{r,2}}{\hat{t}^r_{r,1}} = \frac{\frac{1}{V_2}\frac{\mathrm{d}W_2}{\mathrm{d}x^t}}{\frac{1}{V_1}\frac{\mathrm{d}W_1}{\mathrm{d}x^t}} = \frac{\frac{\hat{t}^r_{r,2}}{V_2}\frac{\mathrm{d}V_2}{\mathrm{d}x^t}}{\frac{\hat{t}^r_{r,1}}{V_1}\frac{\mathrm{d}V_1}{\mathrm{d}x^t}} \tag{26}$$

Equality of the first and last terms of the above equation first yields:

$$\frac{1}{V_1}\frac{\mathrm{d}V_1}{\mathrm{d}x^t} = \frac{1}{V_2}\frac{\mathrm{d}V_2}{\mathrm{d}x^t} \tag{27}$$

So, the fractional volumetric expansion rates are equivalent. Substituting from eqs. (20) and (21) yields:

$$\frac{1}{r_1}\frac{\mathrm{d}r_1}{\mathrm{d}x^t} = \frac{1}{r_2}\frac{\mathrm{d}r_2}{\mathrm{d}x^t} = H \tag{28}$$

And, the isotropic relative linear expansion rates are equivalent. This is the Hubble-Lemaître law.

So, in the *unconditioned* gravitational expansion of space, the Hubble parameter *H is the same everywhere*, irrespective of the separations and the pressures and energy densities of the gravitational field involved, due solely to the non-thermal isobaric nature of the expansion of the invisible gravitational field proposed to underlie the observable spatial expansion.

Therefore, in the expansion, the field conserves its energy density everywhere in pre-existent space, whereby gravitational energy is divergence-free as implied by eq. (17). Yet, in this process, *energy is being created everywhere* in emergent gravitational fields within emergent spaces. So, the gravitational field has a *dynamically* energetic nature: it *grows* by *creating* energy. This behaviour of gravity is a radical departure from those of matter and radiation as, also, is the related *unconditionality* of its conservation of energy density. This singular nature of gravity is explored in the next section.

3.0 Gravitational auto-induction and growth

In presenting his theory of gravitation in [2], Einstein derived his general field equations that represent the 'total system' from his field equations of gravity in the absence of matter and radiation - $R_{\mu\nu} = 0$ - and eq. (11). The quantity $R_{\mu\nu}$ is the Ricci tensor. In so doing, he first arrived at the following relation:

$$\frac{\partial}{\partial x^\alpha}\left(g^{\beta\sigma}\Gamma^\alpha_{\mu\beta}\right) = -\kappa\left(\hat{t}^\sigma_\mu - \frac{\delta^\sigma_\mu}{2}\hat{t}\right) \tag{29}$$

Where, $\hat{t} = \hat{t}^\mu_\mu = tr\{\hat{t}^\sigma_\mu\}$ is the trace of the pseudo-tensors given by the sum of its diagonal elements, the latter given in eq. (16). Then, at this point, Einstein made the remarkable substitutions:

$$\hat{t} \longrightarrow \hat{t} + T \quad \text{and} \quad \hat{t}^\sigma_\mu \longrightarrow \hat{t}^\sigma_\mu + T^\sigma_\mu \tag{30}$$

Where, T^σ_μ is the energy tensor of matter and radiation and T is the trace of the energy tensor of matter (the energy tensor of radiation being traceless). As a result of gravity's isotropy, negative pressure and *EoS*, the trace of its energetic flux densities is given by:

$$\hat{t} = 2\hat{t}^r_r = -2\hat{t}^t_t < 0 \tag{31}$$

So, by means of the substitutions of (30), Einstein then arrived at:

$$\frac{\partial}{\partial x^\alpha}\left(g^{\beta\sigma}\Gamma^\alpha_{\mu\beta}\right) = -\kappa\left[\left(\hat{t}^\sigma_\mu + T^\sigma_\mu\right) - \frac{\delta^\sigma_\mu}{2}(\hat{t} + T)\right] \tag{32}$$

In explaining the substitutions, Einstein offered the following:

'It must be admitted that this introduction of the energy-tensor of matter is not justified by the relativity postulate [of the general covariance of the laws of nature] alone. For this reason, we have deduced it from the requirement that the energy of the gravitational field acts in the same way as other kinds of energy' [2].

The action that Einstein referred to, described in the above equation, is the *induction* of the gravitational field by the energy tensors of matter and radiation and by *energy pseudo-tensors* of gravity. Equation (32) is the *general equation of gravitational induction*.

And, by this pathway, Einstein arrived at his general field equations: $R_{\mu\nu} = -\kappa\left(T_{\mu\nu} - g_{\mu\nu}T/2\right)$. [2]

Einstein's substitutions make explicit a feedback mechanism, actually already present in eq. (29), that drives continuous changes in the field components of gravity and, correspondingly, in its energy components even in the *absence* of energetic fluxes of matter. This is the *dynamical auto-induction of gravity.*

In the exploration of the process of gravitational auto-induction, it is facilitative to ensure the exclusion of external factors by setting the energy tensors in eq. (32) to zero, yielding eq. (29), then rewrite it as:

$$\mathrm{d}\left(g^{\beta\sigma}\Gamma^{\alpha}_{\mu\beta}\right) = -\kappa\left(\hat{t}^{\sigma}_{\mu} - \frac{\delta^{\sigma}_{\mu}}{2}\hat{t}\right)\mathrm{d}x^{\alpha} \tag{33}$$

So, the components of the field that *evolve*, *due only to the passage of time*, are identified by denoting the index α by t in the above equation. Finite changes in these components are obtained by integrating eq. (33), firstly, yielding:

$$\Delta\left(g^{\beta\sigma}\Gamma^{t}_{\mu\beta}\right) = -\kappa\int_{ct_o}^{ct}\left(\hat{t}^{\sigma}_{\mu} - \frac{\delta^{\sigma}_{\mu}}{2}\hat{t}\right)\mathrm{d}x^{t} \tag{34}$$

Multiply by the metric and rewrite as:

$$g_{\beta\sigma}(r,t)g^{\beta\sigma}(r,t)\Gamma^{t}_{\mu\beta}(r,t) = g_{\beta\sigma}(r,t)g^{\beta\sigma}(r_0,t_0)\Gamma^{t}_{\mu\beta}(r_0,t_0) - g_{\beta\sigma}(r,t)\kappa\int_{x_0^t}^{x^t}\left(\hat{t}^{\sigma}_{\mu} - \frac{\delta^{\sigma}_{\mu}}{2}\hat{t}\right)\mathrm{d}x^{t} \tag{35}$$

Within the isotropic coordinate system, the indexes, β and σ for example, no longer indicate generalized coordinates, but permutations of r and t, therefore, $g_{\beta\sigma}(r,t)g^{\beta\sigma}(r,t) = \delta^{\beta}_{\beta} = 1$. Also, as pseudo-tensors do not change in time, then the integrand is time invariant. Therefore, the auto-induced augmented time components of the gravitational field, in the absence of matter and radiation, are given by:

$$\Gamma^{t}_{\mu\beta}(r,t) = g_{\beta\sigma}(r,t)g^{\beta\sigma}(r_0,t_0)\Gamma^{t}_{\mu\beta}(r_0,t_0) - g_{\beta\sigma}(r,t)\kappa\left(\hat{t}^{\sigma}_{\mu} - \frac{\delta^{\sigma}_{\mu}}{2}\hat{t}\right)\Delta x^{t} \tag{36}$$

This equation - that, by its last term, increments the time components of the gravitational field - is the critical regenerative phase of a positive gravitational feedback cycle. It describes the auto-induction of the time components of the field. In this regenerative process, the spatial extents of the time components of the gravitational field *grow* from r_0 to r, as is indicated in eq. (36).

The space components of the gravitational field, in the absence of matter and radiation, undergo similar augmentation triggered not by the passage of time, as in the previous case, but by the spatial extension of the field initiated by the augmented time components of the field. Since, in the expansion, the gravitational field conserves its densities at comoving locations, then this process is described by the preceding development after replacing the index t by r.

The growth of the field described for its time components in eq. (36) - and correspondingly for its space components, for they share the same extents - mathematically implies, according to eqs. (13) and (14), the simultaneous growth of the energy pseudo-tensors and, by means of eq. (31), of their trace, whereby, the regenerative cycle returns to eq. (36) to recommence. Gravitational auto-induction leads to the continuous growth of the field throughout the gravitational manifold. As the gravitational field grows, so does its form - space.

Consider a homogeneous region of the universe undergoing the Hubble expansion without peculiar motions or astrophysical processes that breach its baryonic or radiative contents in total or in composition. The spatial expansion is described by a linear time-varying scale factor $a(x^t)$. Denoting, in eq. (32), α by r and initial

conditions by the subscript 0, then, as the energy tensor of radiation is traceless, there results the following equation describing the rate of growth of the gravitational field over time:

$$\frac{\partial}{\partial x^r}\left(g^{\beta\sigma}\Gamma^r_{\mu\beta}\right) = -\kappa\left\{\hat{t}^\sigma_\mu + T^\sigma_{\mu,0,B}[a(x^t)]^{-3} + T^\sigma_{\mu,0,R}[a(x^t)]^{-4} - \frac{\delta^\sigma_\mu}{2}\left[\hat{t} + T_{0,B}\left(a(x^t)\right)^{-3}\right]\right\} \quad (37)$$

Where, the subscripts B and R indicate baryons and radiation, respectively. The Hubble expansion dilutes the energy tensors of matter and radiation. So, their impacts in the induction of the gravitational field are progressively reduced. However, at comoving locations, the growing gravitational field conserves its energetic flux densities during the coinciding spatial expansion. Therefore, over time, gravity would increasingly dominate matter and radiation in the induction and growth of the gravitational field.

4.0 The gravitational-spatial expansion in the presence of energy tensors

The generic Hubble parameter is given in the relations:

$$H = \dot{a}/a = v/r \quad (38)$$

The equality of the first and last terms constitute the empirical Hubble-Lemaître law. This law holds in homogeneous universes and regions. It may be derived from purely formal considerations, that is, without reference to underlying physics, for example, as in [14]. In §2.3, unconditioned isobaric dynamics of gravity, enabled by the proposition of a spatial form of gravity, led to the Hubble- Lemaître law with an invariant Hubble parameter. This implies that the conditions of gravitational induction and growth, explored in the previous section, may directly impact the expansion of space. Influences of these conditions on the gravitational-spatial expansion will be explored in the following subsections.

4.1 A general Hubble parameter

The field components of gravity are derived *solely* from the invariance of distances across physical space measurable by rods (or time intervals locally measurable by clocks) generally expressed as $\delta(\Delta s) = 0$. [2] So, clearly, *field components of gravity are existentially related to distances* (and proper time intervals). The length of the geodesic line element - $\mathrm{d}s$ - is independent of coordinate systems, although being specified, in equations of line elements, by coordinate intervals and metric components. The components of the gravitational field are functions of components of the inverse metric and of coordinate derivatives of the metric components. The metric, itself, is a function of coordinate derivatives of coordinate intervals. A function of the metric, in the equation of the line element, is to ensure the essential correspondence between coordinate intervals (with determinations influenced by the conditions of measurement) of a coordinate chart and the distance - the invariant length of a line element in physical space. The metric may perform a similar role, in equations of the gravitational field components, of ensuring that these relate, in a direct way, to distances across the field components' physical extents. So, by virtue of complete dependences on a *common* metric, gravity and physical space are *coupled*. This is not inconsistent with an inert expanding 3-D physical space being the *form* of an energetically evolving 4-D field for, by virtue of the shared metric, they have identical spatial extents.

Therefore, if indeed space is the form of the gravitational field, then, eq. (37), that describes the growth of the field due to its induction, may also provide a description of the expansion of physical space over time. Towards this end, in this equation, denote the indices β, σ and μ as t and, as $\delta^t_t = 1$ and eq. (31) implies $\hat{t} = -2\hat{t}^t_t$, then - with the energy tensor of radiation being traceless - eq. (37) may be rewritten as:

$$\mathrm{d}(g^{tt}\Gamma^r_{tt}) = -\frac{\kappa}{2}\left[4\hat{t}^t_t + 2T^t_{t,B} + 2T^t_{t,R} - T_B\right]\mathrm{d}x^r \quad (39)$$

This equation describes the growth of the gravitational field component - Γ^r_{tt}. However, in §5.3.3, it will be shown that the quantity $\Gamma^r_{tt}/g_{tt} = g^{tt}\Gamma^r_{tt}$ is a locally determined *peculiar* geodesic acceleration due to the field component Γ^r_{tt}. It follows that, $\mathrm{d}(g^{tt}\Gamma^r_{tt})$, also, is a locally determined infinitesimal incremental geodesic acceleration. However, it is due only to the growth of the gravitational field: it is an increasing *proper* acceleration. Proper motions of bodies occur *solely* due to their *embedment* in the growing gravitational field. In peculiar motions, bodies

traverse the growing field while being embedded in it. So, here, the expression $\mathrm{d}(g^{tt}\Gamma^r_{tt})$ describes this *coincidence of peculiar and proper gravitational motions*. Since eq. (37) describes the growth of the space components of gravity that follows the growth of the time components of gravity, as described in §3, then such an *accelerating* growth occurs for all field components of gravity. (Though, as will be encountered in §5.3.1, some components are vanishingly faint deep in cosmic voids and indistinct at the large scales of homogeneity.)

Consider this proper motion starting relatively from rest with an increasing acceleration due to the growth of the field that, over the infinitesimal duration $\mathrm{d}x^t$, results in the incremental infinitesimal collinear velocity $\mathrm{d}v$ due to the linear growth $\mathrm{d}r$ of space. The proper acceleration and velocity, in the comoving frame, are generally described as being positive. So, the relative acceleration may be expressed, to a first order, as $|\mathrm{d}(g^{tt}\Gamma^r_{tt})| = \mathrm{d}v/\mathrm{d}x^t = (\mathrm{d}v/\mathrm{d}r)(\mathrm{d}r/\mathrm{d}x^t) = (\mathrm{d}v)^2/\mathrm{d}r = H\mathrm{d}v$. Where, the infinitesimal form of the empirical Hubble-Lemaître law, given in eq. (38), is applied as the spatial expansion is considered, here, as being the form of the growing gravitational field. Substituting from these expressions of the accelerating growth of the gravitational-spatial manifold into eq. (39) and denoting x^r as r yield the Hubble parameter:

$$H = \frac{\mathrm{d}v}{\mathrm{d}r} = \left|\frac{\mathrm{d}(g^{tt}\Gamma^r_{tt})}{\mathrm{d}x^r}\right|^{1/2} = \left[\frac{\kappa}{2}\left(4\hat{t}^t_t + 2T^t_{t,B} + 2T^t_{t,R} - T_B\right)\right]^{1/2} \tag{40}$$

This equation is the Hubble-Lemaître law with a generally applicable expression of the Hubble parameter. It implies that, *at infinitesimal scales*, the energetic induction of gravity gives rise to the growth of the gravitational-spatial manifold at increasing speeds and accelerations, that taken relative to the distance, are equal to the Hubble parameter and its square, respectively.

4.2 The Hubble parameter in the late homogeneous universe

Setting the 3-velocity $u^r = \mathrm{d}x^r/\mathrm{d}s = 0$, then, the energy density flux of matter may be expressed, locally within the FLRW spacetime, as the mixed tensor $T^t_{t,B} = (p_B + \rho_B)u^t u_t - p_B g^t_t$, where p_B and ρ_B are the pressure and rest energy density, respectively, and $\mathrm{g}^t_t = \delta^t_t = 1$. With $g_{tt} = 1$ and $u^r = 0$, then, eq. (2) implies $u^t = \mathrm{d}x^t/\mathrm{d}s = 1$, so, $u_t = g_{tt}u^t = 1$. With the pressure p_B being negligible in the later universe, then, $T^t_{t,B} = T_B = \rho_B$. Also, in the late universe, the radiation density $T^t_{t,R}$ is negligible. Making these substitutions in eq. (40) yields:

$$H = \left\{\frac{\kappa}{2}[4\hat{t}^t_t + \rho_B]\right\}^{1/2} \tag{41}$$

It may be expected that, in a homogeneous universe, pseudo-tensors that do not change with time, also, do not change with location, as is the case in the FLRW universe (cf. §2.2). So, this equation yields the Hubble parameter as:

$$H(x^t) = \left[\frac{\kappa}{2}\left(4\hat{t}^t_t + \rho_{B,0}[a(x^t)]^{-3}\right)\right]^{1/2} \tag{42}$$

This equation recalls, to a factor of $\sqrt{2/3}$, the first Friedmann equation, without curvature, if the term $4\kappa\hat{t}^t_t$ is identified as a gravitational 'cosmological constant' Λ_G with density $\rho_{\Lambda_G} = 4\hat{t}^t_t$.

Recall $a(t) = 1 + z$, where z is the redshift. Differentiate this expression and, with substitution from eq. (38), write as $\mathrm{d}a/\mathrm{d}t = \mathrm{d}z/\mathrm{d}t = (\mathrm{d}z/\mathrm{d}r)(\mathrm{d}r/\mathrm{d}t) = aH = \mathrm{c}(\mathrm{d}z/\mathrm{d}r)$, as the speed of light $\mathrm{c} = \mathrm{d}r/\mathrm{d}t$. The Hubble-Lemaître law may be obtained from $L = ar$, where L is the distance and r is a comoving coordinate interval. [14] So, the infinitesimal linear gravitational growth underlying the spatial expansion is $\mathrm{d}L = a\mathrm{d}r = (\mathrm{c}/H)\mathrm{d}z$. In order to facilitate comparisons with observations, a lookback time frame is assumed. Substitute $a = 1/(z + 1)$ into eq. (42) then substitute the result into the preceding equation:

$$\mathrm{d}L = \frac{\mathrm{c}}{\sqrt{2\kappa\hat{t}_t^t}}\left[1+\frac{\rho_{B,0}}{4\hat{t}_t^t}(1+z)^3\right]^{-\frac{1}{2}}\mathrm{d}z \tag{43}$$

In a universe empty of matter and radiation, or deep in a large void in the late universe, $\rho_{B,0}=0$. In the above equation, this yields $dL=\left[\mathrm{c}/(2\kappa\hat{t}_t^t)^{1/2}\right]\mathrm{d}z$. Here, the absence of energy tensors invokes the isobaric relative expansion rate H of the gravitational-spatial manifold encountered in §2.3 that, notably, is invariant under changes in the pressure $\hat{t}_r^r$ and, therefore, according to eq. (15), also to changes in density $\hat{t}_t^t$. Along with its spatial invariance in the homogeneous universe, this implies the temporal invariance of H in the absence of energy tensors. So, deep in cosmic voids (or in a de Sitter universe), the expansion is described by an invariant Hubble parameter that may be expressed as $H=(2\kappa\hat{t}_t^t)^{1/2}=(\Lambda_G/2)^{1/2}$. As obtained in §2.2, in the homogeneous FLRW universe, $\hat{t}_t^t=H^2/2\kappa$, therefore, the gravitational 'cosmological constant' - Λ_G - has a density of $\rho_{\Lambda_G}=4\hat{t}_t^t=2H^2/\kappa$ or, equivalently, a density parameter of $\Omega_{\Lambda_G}=2/3$. This latter value is moderately lower than the *Planck* 2018 cosmological constant result [15] at about the 2.5σ level. So, in the absence of matter and radiation, there results the de Sitter expansion that, here, is due only to gravity.

It follows, from eq. (42), that the Hubble parameter in the late homogeneous universe may be expressed as:

$$H=\left[\frac{\Lambda_G}{2}+\frac{\kappa}{2}\rho_{B,0}(1+z)^3\right]^{\frac{1}{2}} \tag{44}$$

So, the Hubble constant may be given here as:

$$H_0=\left(\frac{\Lambda_G}{2}+\frac{\kappa}{2}\rho_{B,0}\right)^{1/2} \tag{45}$$

Therefore, both ΛCDM's and de Sitter's cosmological constants may be perceived as symbolic placeholders for the physical gravitational field due to their common invariant impacts in the expansions of homogeneous universes.

Furthermore, as proposed agents of the expansion of our universe, the gravitational 'cosmological constant' Λ_G and the concordance model's cosmological constant Λ have striking similarities. Along with moderately different densities, they have, in common, dynamical barotropic natures, negative pressures and an identical *EoS* parameter $w=-1$ that yields an isobaric spatial expansion with a rate that, taken relative to the linear growth, has a constant H acceleration that is increased in the presence of matter and radiation, and both are invisible ('dark').

5.0 Gravitational-spatial expansion and geodesics

5.1 The gravitationally perturbed Robertson-Walker spacetime

If the spatial expansion - established at large scales across which the universe appears homogeneous - is due to the growth of the gravitational field, then this growth may influence orbits. Such an influence was implied in the last section in the coincidence of the proper infinitesimal incremental linear acceleration $|\mathrm{d}(g^{tt}\Gamma_{tt}^r)|$ - due to the growth of the field component Γ_{tt}^r - and the peculiar acceleration - $\Gamma_{tt}^r/g_{tt}=g^{tt}\Gamma_{tt}^r$ - guided by the same field component. However, in order to describe orbits, the small-scale granular inhomogeneity of bodies must be represented. Such considerations of the coincidence of the proper and peculiar motions of orbiting bodies may be accommodated in a gravitationally perturbed Robertson-Walker (gpRW) spacetime.

The gpRW metric is usually applied in descriptions of the peculiar gravitational motions, against the background of the cosmic Hubble flow, that expresses and enhances incipient cosmological inhomogeneity and lead to gravitational collapse in the earlier universe [16]. Therefore, it is capable of accommodating descriptions of phenomena *simultaneously* involving gravitational attraction and the cosmic recession.

In describing gravitational collapse, the potential term in the gpRW metric usually reflects linear density fluctuations preceding the collapse. [16] However, here, this metric provides an expanding spacetime for gravitational systems associated with spherical bodies including stars, compact bodies and planets, as well as for spherical gravitational systems including solar systems, stellar clusters, spheroidal galaxies and much larger spheroidal agglomerations in the forms of galactic clusters. All these gravitational systems form through

gravitational collapse, exhibit gravitational attraction and curvilinear geodesics while, given the above-mentioned coincidence of their proper and peculiar accelerations, *remaining* in the cosmic recession produced by the growth of the monolithic cosmic gravitational field.

It is its accommodation of orbiting bodies and deflecting radiation that enables the use of the gpRW metric in describing the influence of the expansion on the evolutions of *quasi-Schwarzschild* gravitational systems. Quasi-Schwarzschild gravitating systems, here, imply gravitationally collapsed objects and the curvilinear parts of the expanding gravitational field in which they exist. Such entities, regardless of the morphology of their baryonic distributions, converge to point mass gravitating objects at intermediate distances, while the associated gravitational curvilinearity, more remotely, vanishes asymptotically.

In an isotropic frame, the components of the gpRW metric and its inverse are:

$$g_{rr} = -a^2\left(1+\frac{2\Phi(r)}{\mathrm{c}^2}\right)^{-1} \tag{46}$$

$$g^{rr} = -\frac{1}{a^2}\left(1+\frac{2\Phi(r)}{\mathrm{c}^2}\right) \tag{47}$$

$$g_{tt} = \left(1+\frac{2\Phi(r)}{\mathrm{c}^2}\right) \tag{48}$$

$$g^{tt} = \left(1+\frac{2\Phi(r)}{\mathrm{c}^2}\right)^{-1} \tag{49}$$

Where, $\Phi(r)$ is the gravitational potential.

So, here, the scale factor represents a background expansion stretching physical and, so, coordinate intervals alike, due to the *embedment* of bodies and radiation in the expanding cosmic gravitational-spatial manifold, even during their traversals, so leading to the coincidence of proper and peculiar motions encountered in the last section. The outcomes of such coincidences will be explored here.

The linear expansion may be expressed as the product of the scale factor and an unchanging comoving radial coordinate χ defined as:

$$\chi = r/a \tag{50}$$

This is the radial variable of the FLRW and gpRW line elements.

Explorations, here, of the expansion include geodesics in a void, a model of spherically symmetric gravitating bodies with satellites of infinitesimal masses such as idealized solar systems and an Hernquist analytical model representing spheroidal agglomerations such as galaxies and their clusters.

The state of a gravitational system is taken, here, to be indicated by the radial profiles of its energetic fluxes and the characteristics of its geodesics - radial acceleration and circular speeds of satellites and the speeds and angles of deflection of radiation. The initial states of these evolving gravitational systems are taken to be those existing at times of completion of collapse to form bodies or at times of virialization to form galaxies at which the scale factor is, ideally here, normalized to unity.

In the descriptions that follow, the centroids of gravitating bodies and galactic agglomerations bear the origins of the frames of reference applied and have no peculiar motion.

5.2 Initial gravitational energy densities in gravitational systems

In order to understand the strange kinematics of the satellites and unexpected gravitational optics, consider the influences of the growing gravitational field on orbits and gravitational lenses. For this purpose, the gravitational field is, here, *represented* [11] by its energy density.

The gravitational potential around a spherically symmetric body is given by $\Phi(r) = -\mathrm{G}M/r$. Substituting this, along with the Schwarzschild radius $r_s = 2\mathrm{G}M/\mathrm{c}^2$, into eqs. (46) to (49) yields:

$$g_{rr} = -a^2\left(1-\frac{r_s}{r}\right)^{-1} \tag{51}$$

$$g^{rr} = -\frac{1}{a^2}\left(1 - \frac{r_s}{r}\right) \tag{52}$$

$$g_{tt} = \left(1 - \frac{r_s}{r}\right) \tag{53}$$

$$g^{tt} = \left(1 - \frac{r_s}{r}\right)^{-1} \tag{54}$$

The coordinate first derivatives of the components of the metric are:

$$\frac{\partial g_{rr}}{\partial x^r} = \frac{a^2 r_s}{r^2}\left(1 - \frac{r_s}{r}\right)^{-2} \tag{55}$$

$$\frac{\partial g_{rr}}{\partial x^t} = -2a\dot{a}\left(1 - \frac{r_s}{r}\right)^{-1} + \frac{a^2 \dot{r} r_s}{r^2}\left(1 - \frac{r_s}{r}\right)^{-2} \tag{56}$$

$$\frac{\partial g_{tt}}{\partial x^r} = \frac{r_s}{r^2} \tag{57}$$

$$\frac{\partial g_{tt}}{\partial x^t} = \frac{r_s \dot{r}}{r^2} \tag{58}$$

Substituting from eq. (52) and eqs. (54) to (58) into eqs. (5) to (8) and, subsequently, from this last set and into eq. (14), leads to:

$$\kappa \hat{t}_t^t = \frac{\dot{a}^2}{2a^2}\left(1 - \frac{r_s}{r}\right)^{-1} - \frac{\dot{a}\dot{r} r_s}{2ar^2}\left(1 - \frac{r_s}{r}\right)^{-2} \tag{59}$$

By means of eq. (38), the quotient $\dot{a}/a$ may be replaced by H. Then, in the Hubble flow, both the 'stationary' observer and the locally observed move away from the centre of the spherical body - that serves as the origin of the coordinate chart here applied - at the radial speed given by eq. (38) as:

$$\dot{r} = \frac{\mathrm{d}x^r}{\mathrm{d}x^t} = \frac{1}{\mathrm{c}}\frac{\mathrm{d}r}{\mathrm{d}t} = Hr \tag{60}$$

Where, H is the Hubble parameter in units equivalent to per c seconds and c is the speed of light in the absence of matter. So, with these substitutions, eq. (59) becomes:

$$\hat{t}_t^t = \frac{H^2}{2\kappa}\left[\left(1 - \frac{r_s}{r}\right)^{-1} - \frac{r_s}{r}\left(1 - \frac{r_s}{r}\right)^{-2}\right] \tag{61}$$

This function vanishes at $r = 2r_s$ and becomes negative at lesser radii. For $r > 2r_s$, the density turns out to be positive and directly proportional to the square of the Hubble parameter. It is in these latter regions that the expansion occurs according to the barotropic dynamics of gravity encountered in §2.3. So, in general, descriptions here will be limited to such regions. Panel (a) of fig. 1 shows the initial radial profile of the gravitational energy density. It rises curvilinearly from zero, at $r = 2r_s$, asymptotically attaining a maximal $H^2/2\kappa \sim$ 1.52E-27 $0.66h^2$ kg m^{-3} and becoming flatter (linear), remotely.

With regards to galactic systems, a Hernquist model of a spherically symmetric system - galaxy or galactic cluster - is adopted from [17]. Its matter distribution and potential, respectively, are:

$$\rho(r) = \rho_G\left[\frac{r}{a_G}\left(1 + \frac{r}{a_G}\right)^3\right]^{-1} \tag{62}$$

and

$$\Phi(r) = -\frac{\sigma_G^2}{1 + \frac{r}{a_G}} \tag{63}$$

Where, $\rho_G = \sigma_G^2/2\pi a_G^2$, $\sigma_G = \sqrt{GM_G/a_G}$, M_G and a_G are the characteristic density, characteristic velocity, total mass, and scale length, respectively, of the model.

Substituting from eq. (63) into eqs. (46) to (49), then the components of the metric and its inverse are:

$$g_{rr} = -a^2\left[1-\frac{2\sigma_G^2}{c^2\left(1+\frac{r}{a_G}\right)}\right]^{-1} \tag{64}$$

$$g^{rr} = -\frac{1}{a^2}\left[1-\frac{2\sigma_G^2}{c^2\left(1+\frac{r}{a_G}\right)}\right] \tag{65}$$

$$g_{tt} = 1-\frac{2\sigma_G^2}{c^2\left(1+\frac{r}{a_G}\right)} \tag{66}$$

$$g^{tt} = \left[1-\frac{2\sigma_G^2}{c^2\left(1+\frac{r}{a_G}\right)}\right]^{-1} \tag{67}$$

The coordinate first derivatives of the components of the metric are:

$$\frac{\partial g_{rr}}{\partial x^r} = \frac{2a^2\sigma_G^2}{a_G c^2}\left(1-\frac{2\sigma_G^2}{c^2}+\frac{r}{a_G}\right)^{-2} \tag{68}$$

$$\frac{\partial g_{rr}}{\partial x^t} = -2a\dot{a}\left[1-\frac{2\sigma_G^2}{c^2\left(1+\frac{r}{a_G}\right)}\right]^{-1} + \frac{2a^2\sigma_G^2\dot{r}}{a_G c^2}\left(1-\frac{2\sigma_G^2}{c^2}+\frac{r}{a_G}\right)^{-2} \tag{69}$$

$$\frac{\partial g_{tt}}{\partial x^r} = \frac{2\sigma_G^2}{a_G c^2\left(1+\frac{r}{a_G}\right)^2} \tag{70}$$

$$\frac{\partial g_{tt}}{\partial x^t} = \frac{2\sigma_G^2\dot{r}}{a_G c^2\left(1+\frac{r}{a_G}\right)^2} \tag{71}$$

Substituting from eqs. (60) and (65) and eqs. (69) to (71) into eqs. (5) to (8) and, subsequently, from the latter set into eq. (14), that with the replacement of $\dot{a}/a$ by the Hubble parameter, leads to:

$$\hat{t}_t^t = \frac{H^2}{2\kappa}\left[1-\frac{2\sigma_G^2}{c^2\left(1+\frac{r}{a_G}\right)}\right]^{-1} - \frac{\sigma_G^2 H^2 r}{2a_G\kappa c^2}\left(1-\frac{2\sigma_G^2}{c^2}+\frac{r}{a_G}\right)^{-2} \tag{72}$$

Panel (a) of fig. 2 shows the galactocentric radial energy density profile obtained from eq. (72). As the centroid is approached, the profile declines curvilinearly by < 1.0E-8 of the constant value of $H^2/2\kappa \sim$ 1.52E-27 $0.66h^2$ kg m^{-3} attained remotely where it asymptotically becomes flat.

5.3 Influences of the expansion at small scales

5.3.1 Geodesics in cosmic voids

In these parts, in the limit as $r_s/r \rightarrow 0$, or as $r/a_G \rightarrow \infty$, the equation of the gpRW line element - obtained by substituting eqs. (51) and (53), or (64) and (66), respectively, into eq. (1) - turns out to be similar to that of the FLWR universe:

$$(\mathrm{d}s)^2 = (\mathrm{d}x^0)^2 - a^2\{(\mathrm{d}x^1)^2 + (\mathrm{d}x^2)^2 + (\mathrm{d}x^3)^2\} \tag{73}$$

The common form of the metric of expanding voids and the FLRW universe reflects the homogeneity of the conditions of the expansions. In homogeneous regions, that is, in voids and in the FLRW universe, the potential vanishes as there is no net gravitational attraction. In the FLRW universe, the Hubble parameter decreases with the accompanying dilution of matter. However, (ignoring the extremely rarefied baryonic medium), here deep in the cosmic voids, homogeneity pertains only to the growing gravitational field. This is gravity *acting on its own* - uniformly, isotropically, with a constant *H* relative recession rate, both in growing itself and in expanding space, the latter, just like the cosmological constant.

So, unlike static curvilinear spacetimes, the gpRW spacetime does not asymptotically vanish remote from bodies to be replaced by a Minkowskian spacetime that is without gravity (Birkhoff's theorem [18]). Instead, in regions remote from bodies, where $r_s/r \rightarrow 0$, or $r/a_G \rightarrow \infty$, the field is most energetic, with maximum magnitudes of energy density, (as shown in §5.2) and pressure. So, these are not regions of the vacuum (as addressed by Birkhoff's theorem), but are domains, remote from matter, in an energetic and dynamical fluidic gravitational field of a 'fluid filled' spacetime [18]. The significantly greater portion of the observable universe consists of large spaces almost empty of baryons [19]. Therefore, the maximal flatness and energy intensity of the field prevail over the significantly greater portion of the observable universe.

Equation (73) implies that null geodesics in the voids are rectilinear and the velocity of light, locally undiminished, apparently reduces with increasing distance along the line of sight from the observer according to the relation $\gamma = \mathrm{d}x^r/\mathrm{d}x^t = \pm 1/a = \pm(1+z)^{-1}$. This occurs due to the extension of the distance between comoving observer and target, or emitter, due to the expansion of the gravitational-spatial manifold in cosmic voids during the flight of photons.

In vast voids surrounding regions of static curvilinear spacetimes, the vanishing of the coordinate derivatives of the components of the metric in eq. (11) implies vanishing gravitational fields. However, in the dynamic 'fluid filled' [18] gpRW spacetime, the quantity $\partial g_{rr}/\partial x^t$, remote from bodies, approaches a non-zero value. So, for the field around spherical bodies, eqs. (52), (56) and (7) yield:

$$\Gamma^{\mathrm{r}}_{\mathrm{tr}} = -\frac{\dot{a}}{a} + \frac{\dot{r} r_s}{2r^2}\left(1 - \frac{r_s}{r}\right)^{-1} \tag{74}$$

Substituting from eqs. (38) and (60) yields:

$$\Gamma^{\mathrm{r}}_{\mathrm{rt}} = -H + \frac{H r_s}{2r}\left(1 - \frac{r_s}{r}\right)^{-1} \rightarrow -H \;: r_s/r \rightarrow 0 \tag{75}$$

In the case of the field related to spheroidal galaxies, eqs. (7), (65) and (69) yield:

$$\Gamma^{\mathrm{r}}_{\mathrm{rt}} = -\frac{\dot{a}}{a} + \frac{\sigma_G^2 \dot{r}}{a^2 a_G \mathrm{c}^2}\frac{1}{\left(1 + \frac{r}{a_G}\right)}\left(1 - \frac{2\sigma_G^2}{\mathrm{c}^2} + \frac{r}{a_G}\right)^{-1} \tag{76}$$

Substitute from eqs. (38) and (60):

$$\Gamma^{\mathrm{r}}_{\mathrm{rt}} = -H + \frac{\sigma_G^2 H r}{a^2 a_G \mathrm{c}^2}\frac{1}{\left(1 + \frac{r}{a_G}\right)}\left(1 - \frac{2\sigma_G^2}{\mathrm{c}^2} + \frac{r}{a_G}\right)^{-1} \rightarrow -H \qquad : r/a_G \rightarrow \infty \tag{77}$$

It is this field component, as shown by its presence in eqs. (13) and (14) amidst the vanishing faintness of the others, that gives rise to the high gravitational pressures and energy densities in these regions remote from bodies.

The existence of the gravitational field in cosmic voids and in the FLRW universe where the gravitational potential vanishes implies that the latter does not characterize the gravitational field, but only applies in

gravitationally curvilinear regions in the vicinities of inhomogeneous matter. The gravitational field is most intense in the absence of matter and the potential.

Consider the geodesic 3-acceleration of bodies guided by the field component $\Gamma^{\mathrm{r}}_{\mathrm{rt}}$ given by:

$$\frac{\mathrm{d}^2x^r}{\mathrm{d}s^2} = \Gamma^{\mathrm{r}}_{\mathrm{rt}}\,\frac{\mathrm{d}x^r}{\mathrm{d}s}\frac{\mathrm{d}x^t}{\mathrm{d}s} \tag{78}$$

Substitute from equations (3), (64) and (75), or (77), as well as, $x^t = ct$ and $\mathrm{d}s = c\mathrm{d}\tau$, and rewrite the equation above as:

$$\frac{1}{c^2}\frac{\mathrm{d}^2r}{\mathrm{d}\tau^2} = -H\frac{\mathrm{d}r}{\mathrm{d}x^t}\left(\frac{\mathrm{d}t}{\mathrm{d}\tau}\right)^2 \tag{79}$$

Then, with $v = \mathrm{d}r/\mathrm{d}x^t$, rewrite eq. (40) as $\mathrm{d}v/\mathrm{d}r = (\mathrm{d}v/\mathrm{d}x^t)(\mathrm{d}x^t/\mathrm{d}r) = H$ so that $\dot{v} = H(\mathrm{d}r/\mathrm{d}x^t)$ and rewrite the equation above as:

$$\frac{\mathrm{d}^2r}{\mathrm{d}\tau^2} = -\frac{\mathrm{d}^2r}{\mathrm{d}t^2}\left(\frac{\mathrm{d}t}{\mathrm{d}\tau}\right)^2 \tag{80}$$

On the right of this last equation, the first factor is the *apparent* acceleration of the receding target that is remotely obtained by the observer. It is accompanied by a *coordinate time transformation* that corrects this apparent acceleration to obtain the actual acceleration of the target, given on the left, that is directly measurable locally, in principle, as indicated by the presence of the locally determinable proper time interval $\mathrm{d}\tau$, as opposed to the remotely determined coordinate time interval $\mathrm{d}t$ that may vary with frames of reference.

Similarly, the infinitesimal vector displacement due to the recession, remotely observable as the coordinate radial vector interval $\mathrm{d}r$, is locally observed at the target as the physical displacement $-\mathrm{d}D$. (This may be obtained at the target in the time slice $\mathrm{d}x^0 = 0$ taken at the time of emission of the signal $t = 0$, when $a = 1$, from the equation of the space-like line element obtained from eq. (73) of the time-like line element, with a substitution from eq. (2), by negation of the coefficients of coordinate vector intervals, and then denoting $\mathrm{d}s$ as $-\mathrm{d}D$.) The differences in notation and sign between $\mathrm{d}r$ and $-\mathrm{d}D$ encode, respectively, the difference in proximity to the target - remote and local - and that of the relative orientation - facing - of two observers of the same interval. Making these changes in (80) yields:

$$\frac{\mathrm{d}^2D}{\mathrm{d}\tau^2} = \frac{\mathrm{d}^2r}{\mathrm{d}t^2}\left(\frac{\mathrm{d}t}{\mathrm{d}\tau}\right)^2 \tag{81}$$

This is the Hubble acceleration observed remotely where $\mathrm{d}t/\mathrm{d}\tau > 1$ and locally where $\mathrm{d}t = \mathrm{d}\tau$. Similar considerations attend the determination of the locally measured speed of recession, directly obtainable at the target and that is to be determined by the remote observer, given as:

$$\frac{\mathrm{d}D}{\mathrm{d}\tau} = \frac{\mathrm{d}r}{\mathrm{d}\tau} = \frac{\mathrm{d}r}{\mathrm{d}t}\frac{\mathrm{d}t}{\mathrm{d}\tau} \tag{82}$$

So, in order to remotely obtain the locally measurable speed or acceleration of the target, $\mathrm{d}t/\mathrm{d}\tau$ must be determined. This time transformation reflects the changes observed remotely, by means of an electromagnetic signal, by a distant observer with the aid of an oscillator (clock) in her location, of the apparent time rate (relative to an affine parameter), as remotely determined, of the target's oscillator (source of electromagnetic radiation) relative to its locally determined time rate (that, fortunately, is reproducible in the observer's location). These changes occur to the radiation, as it travels from the emitter to the observer, due to it being *embedded in the expanding field* (as opposed to just noninteractively traversing empty space): as the wavevector is being *stretched*, the consequent extension of the wavelength leads to the frequency decreasing; the radiation redshifts. (In regions of curvilinear gravitational fields, this embedment of radiation leads to gravitational lensing that will be discussed in §5.3.6).

Denote the parameters of the wave produced by the emitting oscillator by the subscript e and measurements of them by means of the observer's oscillator by o. Now, since the time rate is proportional to the period and, thereby, to the wavelength, then:

$$\frac{\mathrm{d}t}{\mathrm{d}\tau} = \frac{\lambda_o}{\lambda_e} = \frac{\lambda_o - \lambda_e}{\lambda_e} + 1 = z + 1 \tag{83}$$

Where, $z = (\lambda_o - \lambda_e)/\lambda_e$ is the fractional change in wavelength that occurs during transmission due to the embedment of radiation in the expanding gravitational-spatial manifold - the cosmological redshift. Therefore, by spectroscopically determining z, the transformation $\mathrm{d}t/\mathrm{d}\tau$ is obtained and by means of eqs. (81) and (82), the actual acceleration and speed, respectively.

Furthermore, note that as the wavelength changes due to the Hubble expansion, then:

$$\frac{\mathrm{d}t}{\mathrm{d}\tau} = \frac{\lambda_o}{\lambda_e} = a = 1 + z \tag{84}$$

Therefore, the scale factor $a(x^t)$ not only dilates space, but also dilates time. It is a linear and homogeneous space and time transformation.

So, it is the field component $\Gamma^{\mathrm{r}}_{\mathrm{rt}}$ that, in the vast voids, governs the linear isotropic geodesic recession of bodies resulting from the metric expansion of space. Here, the geodesic acceleration due to $\Gamma^{\mathrm{r}}_{\mathrm{rt}}$, in cosmic voids, yields the scale factor and the constant Hubble parameter, as well as, the cosmological redshift that characterize the rectilinear null geodesics in these vast regions.

In these gravitationally flat, cumulatively dominant, regions - almost empty of baryons - there occurs the *conflation* of the incompressible expanding fields associated variously with remote bodies in the vicinities of which the fields are curvilinear. The result is that, cosmically, gravitational curvilinearity appears as isolated, widely dispersed and purely local departures, in the vicinities of similarly dispersed bodies and virialized agglomerations of matter, from a flat *cosmic* field.

5.3.2 Accelerating recession of bodies in free fall

Consider the isotropic geodesic 3-acceleration:

$$\frac{\mathrm{d}^2 x^r}{\mathrm{d}s^2} = \Gamma^{\mathrm{r}}_{\mathrm{tt}} \frac{\mathrm{d}x^t}{\mathrm{d}s}\frac{\mathrm{d}x^t}{\mathrm{d}s} + \Gamma^{\mathrm{r}}_{\mathrm{rr}} \frac{\mathrm{d}x^r}{\mathrm{d}s}\frac{\mathrm{d}x^r}{\mathrm{d}s} + \Gamma^{\mathrm{r}}_{\mathrm{rt}} \frac{\mathrm{d}x^r}{\mathrm{d}s}\frac{\mathrm{d}x^t}{\mathrm{d}s} \tag{85}$$

Set $\mathrm{d}x^t/\mathrm{d}s = 1$ so that eq. (2) may be rewritten as $(\mathrm{d}x^r/\mathrm{d}s)^2 = (1 - g_{tt})/g_{rr}$. Substitute from eqs. (51) and (53) into this last equation and from the resulting equation and into (85). Now, substitute from eqs. (52), (55) and (57) and into eqs. (5), (7) and (9), then from these last three and into (85). Then, initializing the system's expansion by normalizing the scale factor at $a = 1$, the acceleration may be expressed as:

$$\frac{\mathrm{d}^2 r}{\mathrm{d}s^2} = -\frac{r_s}{2r^2} - \frac{r_s^2}{2r^3} + H\dot{D}\left(1 - \frac{r_s}{2r}\right) \qquad : r = a(\chi - 2r_s) + 2r_s > 2r_s \tag{86}$$

The first term, on the right, is the attractive Newtonian acceleration. The potential corresponding to the second attractive acceleration term is $-r_s^2/4r^2$. With $r_s = 2\mathrm{G}M/\mathrm{c}^2$ and $r_s/2r = \dot{r}_{rot}^2 = (L/mcr)^2$ - where, $\dot{r}_{rot}$ is the circular speed and L and m are the angular momentum and mass of the satellite, respectively - substituted into the potential term, it becomes $-L^2\mathrm{G}M/m^2\mathrm{c}^4r^3$. This term is recognizable as the relativistic potential that gives rise to the precession of orbits. The last acceleration term of eq. (86) describes the recessional Hubble acceleration. It is obtained by setting $\mathrm{d}r = -(1 - r_s/2r)\mathrm{d}D$ - for the same reasons $\mathrm{d}r$ was set to $-\mathrm{d}D$ in eqs. (81) and (82) and to describe the apparent contraction of the spatial coordinate interval in the presence of inhomogeneous matter distribution that gives rise to the potential expressed, here, as $-r_s/2r$ - then dividing by $\mathrm{d}x^t$ to yield $\dot{r} = -(1 - r_s/2r)\dot{D}$ and substituting $\dot{a}/a = H$ from eq. (38).

Equation (86) explicitly includes *all* isotropic geodesic accelerations - peculiar and proper - and applies at *all scales*. However, the potential and the attractive accelerations become faint remote from gravitating bodies and

recessional accelerations are faint across quasi-Schwarzschild systems. The equation shows that, in small-scale regions in the vicinities of central gravitating bodies, the Hubble expansion occurs along with the orbits. However, here, the relatively small distances and the relatively large peculiar curvilinear motions challenge observations of the expansion. Yet, the peculiar motions bear the imprint of the expansion in the *unexpected stretching* of their curvilinear geodesics due to the Hubble acceleration - $H\dot{D}$, as locally determined. This effect may be integrally obtained by applying the inverse coordinate time transformation $1/a(x^t)$ to the spatial variables in the terms on the right of (86). With eq. (50), this leads to the vanishing of the additive Hubble term as $-(1 - r_s/2r)\dot{D}/\mathrm{a} = \dot{r}/a = \mathrm{d}\chi/\mathrm{d}x^t = 0$. However, in effect, the Hubble acceleration reappears in the attractive terms that, similarly transformed, also directly express the Hubble recession. So, the Hubble expansion results in *extremely slowly extending orbits of constant radial accelerations* given by:

$$\frac{\mathrm{d}^2 r}{\mathrm{d}s^2} = -\frac{a^2 r_s}{2r^2} - \frac{a^3 r_s^2}{2r^3} \qquad : r = a(\chi - 2r_s) + 2r_s > 2r_s \tag{87}$$

That is, natural satellites move under *coinciding contradictory* influences of attraction and recession due to a dialectical gravitational field. This outcome was already heralded in the coincidence of the proper and peculiar accelerations encountered in the previous section. The result is that the peculiar accelerations *retain* their values, established when $a = 1$ and $r = \chi$, during the metric expansion of the gravitational-spatial manifold. So, although coinciding, the peculiar acceleration and the proper acceleration are independent of each other. Here, the only impact of the coincidence of accelerations is that the radii of orbits increase as geodesics are isotropically stretched.

In vast, almost empty, spaces - across which quasi-Schwarzschild systems appear as points of light - the attractive acceleration terms and the potential in eq. (86) become vanishingly small leaving the Hubble acceleration effectively bare and, in principle, readily discernible.

Unlike the attractive peculiar accelerations that are due to interactions of the field and bodies - as in the inducement, by bodies, of curvilinearities in the field and the latter's guidance of bodies and radiation in curvilinear geodesics - the linear isotropic accelerating recessions result from the self-interactions of a cosmic gravitational field - described in §2.3, §3 and §4 - enhanced in the presence of matter and radiation.

In following subsections, the evolutions of circular orbits due only to the gravitational-spatial expansion are further explored.

5.3.3 Initial circular orbits

The circular speed of a satellite around a spherically symmetric body is given by the square root of the product of the magnitude of the Newtonian acceleration term of eq. (86) and the radius expressed, here, as:

$$v_{rot} = \frac{\mathrm{d}r}{\mathrm{d}\tau} = \left| r\frac{\mathrm{d}^2 r}{\mathrm{d}\tau^2} \right|^{\frac{1}{2}} = \left[\frac{\mathrm{c}^2 r_s}{2r} \right]^{\frac{1}{2}} \qquad : r > 2r_s \tag{88}$$

Panel (b) of fig. 1 shows the Keplerian profile of the initial rotation curve in the vicinity of the gravitating body obtained by means of eq. (88).

In regards to the Hernquist galaxy, consider the geodesic equation:

$$\frac{\mathrm{d}^2 x^\tau}{\mathrm{d}s^2} = \Gamma^\tau_{\mu\nu} \frac{\mathrm{d}x^\mu}{\mathrm{d}s} \frac{\mathrm{d}x^\nu}{\mathrm{d}s} \tag{89}$$

Locally, the acceleration may be obtained by setting:

$$\frac{\mathrm{d}x^\mu}{\mathrm{d}s} = \frac{\mathrm{d}x^\nu}{\mathrm{d}s} = 0 \quad : \mu, \nu = 1, 2, 3 \tag{90}$$

In these conditions, eqs. (1) and (66) yield:

$$\frac{\mathrm{d}x^{\mu}}{\mathrm{d}s}=\frac{\mathrm{d}x^{\nu}}{\mathrm{d}s}=\sqrt{\frac{1}{g_{tt}}}=\left[1-\frac{2\sigma_G^2}{\mathrm{c}^2\left(1+\frac{r}{a_G}\right)}\right]^{-\frac{1}{2}}\ :\ \mu,\nu=0 \tag{91}$$

So, with these determinations, eq. (89) yields:

$$\frac{\mathrm{d}^2x^{\tau}}{\mathrm{d}s^2}=\frac{1}{g_{tt}}\Gamma_{tt}^{\tau}\quad :\ \tau=1,2,3 \tag{92}$$

These components of the 3-acceleration may be vectorially summed as:

$$\frac{\mathrm{d}^2x^{r}}{\mathrm{d}s^2}=\frac{1}{g_{tt}}\Gamma_{tt}^{r} \tag{93}$$

This is the locally determined peculiar acceleration of bodies guided by the field component Γ_{tt}^{r}. With this acceleration so described, then substituting from eqs. (65) and (70) into (9) and then from eqs. (9) and (66) and into eq. (93), the radial acceleration may be expressed as:

$$\frac{\mathrm{d}^2x^{r}}{\mathrm{d}s^2}=\frac{1}{\mathrm{c}^2}\frac{\mathrm{d}^2r}{\mathrm{d}\tau^2}=-\frac{\sigma_G^2}{a^2a_G\mathrm{c}^2\left(1+\frac{r}{a_G}\right)^2} \tag{94}$$

And, with $a=1$, the initial circular speed is obtained as:

$$v_{rot}=\frac{\mathrm{d}r}{\mathrm{d}\tau}=\left|r\frac{\mathrm{d}^2r}{\mathrm{d}\tau^2}\right|^{\frac{1}{2}}=\left[\frac{\sigma_G^2r}{a_G\left(1+\frac{r}{a_G}\right)^2}\right]^{\frac{1}{2}} \tag{95}$$

Panel (b) of fig. 2 shows the initial rotation curve of a Hernquist galaxy obtained by means of the equation above.

The rotation curves of Panels (b) of figs. 1 and 2 are velocity profiles of these systems at initiation, when $a=1$. As the gravitational field evolves, the resulting velocity profiles become more remotely connected to the gravitating bodies that initially shaped their curvilinearity. Therefore, unexpected velocity profiles may be due to the unexpected evolution of the gravitational field in the vicinities of gravitating bodies.

5.3.4 Evolution of curvilinear gravitational systems

The square root of the product of the magnitude of the Newtonian acceleration term of eq. (87) and the radius, with radial variables transformed by $1/a$ - as in §5.3.2 - yield the circular speed of a satellite around a spherically symmetric gravitating body at a radius r as:

$$v_{rot}=\left[\frac{a\mathrm{c}^2r_s}{2r}\right]^{\frac{1}{2}}\qquad :r=a(\chi-2r_s)+2r_s>2r_s \tag{96}$$

In effect, the metric expansion does not influence the peculiar kinematics characterized by the circular speed and the radial acceleration, the last as described in eq. (87). This results in *radially stretched* rotation curves becoming more extended at higher scale factor values, as is illustrated in fig. 1.

Energy conservation laws of gravity imply the retention, in the isobaric expansion of the gravitational-spatial manifold, of the value of the gravitational energy density at a comoving location [cf. §2.3]. Therefore, gravitational energy pseudo-tensors, here, are not projected across an interval of time by a metric operation, but - at comoving locations and as time passes - simply retain their initial values, established at $a=1$. This, *naturally*, avoids violations, by the pseudo-tensors, of the coordinate condition - $\sqrt{-g}=a=1$ - that arose in §2.2. As the pseudo-tensors, at comoving locations, do not change during the expansion, then they may be described by functions of a comoving radial variable. So, in the expansion, the gravitational energy density may be obtained from eq. (61) as:

$$\hat{t}_t^t = \frac{H^2}{2\kappa}\left[\left(1-\frac{ar_s}{r}\right)^{-1} - \frac{ar_s}{r}\left(1-\frac{ar_s}{r}\right)^{-2}\right] \qquad : r = a(\chi - 2r_s) + 2r_s > 2r_s \tag{97}$$

Figure 1 shows the progression of a rotation curve and a gravitational energy density radial profile around a compact body for successively larger values of the scale factor. They were produced by means of the applications of eqs. (96) and (97).

There is an ongoing smooth reduction of the gradients as the regions of curvilinear gravity expands in the vicinity of the spherical body. The energy density rises from being vanishingly small at $r = 2r_s$ to asymptotically attaining a maximum of $H^2/2\kappa \sim$ 1.52E-27 $0.66h^2$ kg m^{-3}, remotely.

In the case of an Hernquist system, the incremental proper acceleration, locally determined in §4.1 as $\mathrm{d}[g^{tt}\Gamma^{\mathrm{r}}_{\mathrm{tt}}]$, may be expressed as $H\dot{D}$. In the galactocentric frame, it occurs radially and, therefore, is orthogonal to the peculiar transverse circular velocity v_{rot} due to the peculiar radial acceleration. So, the peculiar velocity is not directly impacted by the proper acceleration. The peculiar acceleration $\Gamma^{\mathrm{r}}_{\mathrm{tt}}/g_{tt}$ is also unaffected by the proper acceleration. This may be obtained by the sum of the locally determined Hubble acceleration $H\dot{D}$ and the locally determined peculiar acceleration given in eq. (94), initialised at $a = 1$, undergoing the inverse time coordinate transformation $1/a(x^t)$, as in §5.3.2. Therefore, the peculiar circular speed is undisturbed by the expansion and may be described by functions of the comoving radius r/a as:

$$v_{rot} = \left[\frac{\sigma_G^2 r}{a_G a\left(1+\frac{r}{a_G a}\right)^2}\right]^{\frac{1}{2}} \tag{98}$$

With regard to the gravitational energy density, its conservation requires that in the expansion it is described by substituting the radial variable in eq. (72) by the comoving radius r/a yielding:

$$\hat{t}_t^t = \frac{H^2}{2\kappa}\left[1-\frac{2\sigma_G^2}{\mathrm{c}^2\left(1+\frac{r}{a_G a}\right)}\right]^{-1} - \frac{\sigma_G^2 H^2 r}{2a_G a\kappa \mathrm{c}^2}\left(1-\frac{2\sigma_G^2}{\mathrm{c}^2}+\frac{\mathrm{r}}{a_G a}\right)^{-2} \tag{99}$$

Figure 2 shows, in a galactocentric frame, the progressions, at increasing values of the scale factor, of a rotation curve and a gravitational energy density radial profile of a spheroidal galaxy. These series were produced by means of the applications of eqs. (98) and (99).

So, here, energy pseudo-tensors, orbital accelerations and circular velocities may be considered as functions purely of the comoving radial coordinate.

The initial profile of the energy density of gravity obtained is almost flat. In approaching the galactic centre, it declines slightly by < 1.0E-8 of its almost constant value of $H^2/2\kappa \sim$ 1.52E-27 $0.66h^2$ kg m^{-3} that prevails remote from the galactic centre. The initial matter distribution determines the initial shape of the field. As the scale factor increases, the initial profile becomes progressively stretched. So, over time, the field changes shape due solely to the expansion and the profiles become steeper in the outer regions.

As the density across a galaxy varies with radius and time, then, in the vicinities of the galaxy the expansion rate varies accordingly. Equation (62) shows that the matter density declines with increasing radius and eq. (41) shows that this results in the Hubble parameter decreasing at increasing radii. That is, the relative linear expansion rates - $H(r,t) = (\mathrm{d}r/\mathrm{d}t)/\mathrm{d}r$ - in the outer regions of the galaxy are lower than those in denser inner regions. However, integrated over the radius, the proper radial speeds v are lower in the inner regions compared to those in the outer regions. So, in these inhomogeneous regions, the scale factor is a function both of space and time variables. Therefore, these profiles, taken at common constant scale-factor cross-sections, are not to be taken as time-lapsed illustrations. However, this does not affect comoving radii nor, thereby, eq. (99).

There is some resemblance of the rotation curves of fig. 2 to those of different galaxies. Such galaxies may just be at different stages in similar patterns of evolution. This evolution will be further explored in the next sub-section.

5.3.5 Gravitational-spatial expansion and apparent dynamic masses of galaxies

Figure 3 illustrates the incremental change in the rotation curve of a galaxy due only to the expansion of the gravitational-spatial manifold. In outer regions, the later profile (dashed curve) shows higher speeds than those of the initial profile (solid curve). The dash-dot line traces the real results of the subtraction, in quadrature, of the speeds of the initial profile from those of the later one.

A profile similar to the later (dashed) one, obtained where one similar to the earlier (solid) profile was expected, may be explained as being due to DM, with higher densities than the luminous matter in the outer regions, giving rise to a component that may be roughly similar to that traced by the dash-dot curve but fitted to rise from the centre. Such fittings generally are weakly constrained [20], especially as the centroids are approached (permitting the 'cusp-core problem' [21]).

Equations (96) and (98) show, respectively, that the circular speeds may be expressed, in fields around spherical gravitating bodies, as $\sqrt{(GMa/r)}$ and in Hernquist galaxies, for $r \gg a_G$, approximately as $\sqrt{(GM_G a/r)}$, where, M and M_G are the masses of baryonic matter. (This demonstrates the quasi-Schwarzschild convergence of the expanding Hernquist system.) In both cases, the velocity profiles, over time, become higher in the outer regions, (cf. figs. 1 and 2) and even rising, as in Panel (h) of fig. 2. Such a development in velocity profiles may be taken to be evidence of increasing dark matter densities. For example:

'The most surprising new result is that the projected rotation velocities [of the selected high redshift galaxies] … reach a maximum … and decrease further out… The six rotation curves drop to $v(R_{out})/v_{max}$~0.3 to 0.9 at the outermost radius sampled.' 'Falling rotation curves have previously been detected at low redshift … although these are rare and drops are modest, to v/v_{max}~0.8-0.95…'. 'Dark matter fractions drop with increasing redshift from 0.8-2.6…'. [22]

So, the *effects* in the outer regions of the expansions of quasi-Schwarzschild systems are *apparently equivalent* to the presence of gravitating masses of Ma and $M_G a$. Therefore, the product of mass and scale factor may be regarded as the *apparent dynamic mass* of a body or of a virialized agglomeration of bodies of a common scale factor. (For a galaxy with k bodies, each possibly with differing scale factors a_i, and total mass $M_G = \Sigma_i M_i$, for ,$i = 1, \ldots k$, the total apparent dynamic mass is $\Sigma_i M_i a_i$, as will be elucidated in §6. In this case, an effective scale factor may be $\Sigma_i M_i a_i / \Sigma_i M_i$.) The assumed extra mass, apparently invisible, may be attributed to DM of apparent dynamic mass fraction $(a-1)/a$. So, the growing curvilinear field offers an alternative explanation to the presence of DM for the extended flattened and even rising rotation curves in outer galactic regions.

Quasi-Schwarzschild gravitational systems, at comoving locations, have constant circular speeds that radially asymptote to $v = (GM_G a/r)^{1/2}$. Additionally, in these locations, the radial accelerations asymptote to $a_r = GM_G a^2/r^2$. Therefore, in these regions, $v^4 = GM_G a_r = (GM_G a/r)^2$. This relation recalls - and appropriately constrained may explain - the empirically established baryonic Tully-Fisher relation (BTFR); $v^4 \propto M_G$ [23]. Therefore, applying eq. (50), express the acceleration as $a_r = GM_G/\chi^2$. Then, under variations of M_G and χ, fixing $da_r = 0$ yields $\chi^2 = M_G$ and $a_r = G$. In this condition, $v^4 = G^2 M_G$ and the BTFR holds. So, with the baryonic mass of the galaxy M_G and its apparent dynamic mass fraction $f_B = 1/a$ determined, then the BTFR is obtainable at the radius $r = M_G^{1/2}/f_B$. Here, $dv/dr = -G^{1/2}/2aM_G^{1/4} \approx 0$ yields the almost 'flat velocity'.

The generally scale dependent quasi-Schwarzschild radially asymptotic relation $v^4 = GM_G a_r$ has a form similar to that of the mass-asymptotic speed relation (MASR) of modified Newtonian dynamics (MOND) [24]. However, in order to produce the direct proportionality of the scale-invariant BTFR here, instead of Milgrom's *fitted* 'fundamental constant' termed the acceleration scale $a_0 = 1.2\text{E-}10$ m s^{-2} [24], there is the radial acceleration - numerically equivalent to Newton's constant - $a_r = G \sim 6.67\text{E-}11$ m s^{-2}. Note that these values are almost of the same order of magnitude: ~ 0.25 dex.

The BTFR 'has been studied intensively by various groups ... and has been found to apply with smaller scatter than the original TFR to both HSB (high surface brightness) and LSB (low surface brightness) spiral galaxies, as well as irregular ... and dwarf irregular galaxies ... covering ~ 5 decades of mass scale: $M_{bar} = 10^{6\sim11} M_\odot$.' [25]

The baryonic Faber-Jackson relation (BFJR) $M_{bar} \propto \sigma^n$, where σ is the velocity dispersion of a pressure supported galaxy of mass M_{bar}, is an empirically established relation that is similar to the BTFR of rotationally supported galaxies:

'when data for elliptical galaxies ... and globular clusters ... are plotted together, the data is seen to cluster along an $n = 4$ line spanning 8 decades of mass scale: $M_{bar} = 10^{4\sim12} M_{\odot}$. And just as in the BTFR, $n = 4$ would immediately imply the existence of an acceleration scale $a_{\emptyset} = \sigma^4/\mathrm{G}M_{bar}$, which is universal among pressure supported systems including elliptical galaxies and globular clusters. Furthermore, the slope found ... from a fit ... implies $a_{\emptyset} \sim O\ 10^{-10}$ m/s^2. Thus, the BTFR and the BFJR together seem to point to the existence of an acceleration scale of order 10^{-10} m/s$^2 \equiv a_{\emptyset}$, which is universal to both rotation and pressure supported systems including and below the galaxy scale. Again, we emphasize that we are discussing observational facts, independent of any theoretical considerations.' [25]

'We see that the 62 data points … cluster around $\sigma^4/\mathrm{G}a_0 = M_{bar}$ … indicating that a_0 also appears in the dynamics of galaxy clusters.' [25]

'With galaxy clusters, galaxies, and globular clusters all included in the plot, we see that the BFJR with $n = 4$ applies to 10 decades of mass scale: $M_{bar} = 10^{4\sim14} M_{\odot}$.' [25]

Note that since the expansion does not change the velocities, then it also does not change their dispersion. Therefore, just as for the BTFR, the BFJR is not affected by the expansion nor by the hypothetical DM. So, the generality of the quasi-Schwarzschild nature of gravitationally bound agglomerations may explain the similarity of the BTFR and BFJR as well as their common 'acceleration scale'.

That the empirically established BTFR and BFJR both *exclude* DM may be due to the latter merely being an *ansatz* of a causation of extended orbits that may actually be due to the expansion of curvilinear parts of the gravitational-spatial manifold. So, it is significant that Mosleh *et al.* [26] may have presented *strong evidence,* from 1000 galaxies*,* of the *expansions of gravitationally bound systems*:

'At all mass bins, the most significant changes of their mass profiles can be seen in the outer regions of these galaxies, i.e., quiescent galaxies at low-z have extended stellar mass profiles compared to their counterparts at high-z.' [26]

This may be due, in part, to accretion in outer parts of the galaxies. [26] However,

'At fixed mass, quiescent galaxies have higher surface densities in the past compared to their counterparts in the local Universe. This evolution scales as $(1+z)^{2.35\pm0.24}$ for massive quiescent galaxies and is similar for lower mass bins.' [26]

So, along with the accretion, there appears to be reductions of the stellar densities that, likely, are due to the expansions of the galaxies. Note that such expansions overall are greater than the cosmic average, as may be expected in overdense regions.

'The central densities decline slightly and the rate of evolution is slow, $\Sigma_{1\ \mathrm{kpc}} \propto (1+z)^{0.55\pm0.08}$ for massive quiescent galaxies, from $z \sim 2$ to $z \sim 0$. This indicates that the central regions of the massive quiescent galaxies were slightly denser at higher redshifts compared to their counterparts at low-z.' [26]

This may be due to infall of stars and gas into the central regions that would tend to offset the reduction of densities due to expansions in these regions. (These higher central stellar concentrations in central regions may, conceivably, lead to expectations, at the time of the later profile, of the earlier profile in fig. 3 discussed above.)

Nevertheless, the evidence strongly supports intragalactic gravitational-spatial expansions.

Huang *et al.* [27] may not only have presented similar evidence of the Hubble expansions of gravitationally bound systems but, crucially, also of a *relation of the expansions with the purely apparent dynamic masses* of so-called DM haloes. They report that:

'With the help of deep images and the redMaPPer cluster catalog... we find evidence that the surface stellar mass density profiles ($\mu_{\star}$) of massive central galaxies depend on dark matter halo mass: central galaxies in more massive halos tend to have more extended stellar mass distributions... and less mass in the inner 10 kpc ($M_{\star}^{10}$).' [27]

'Using data from the HSC survey, we perform careful aperture mass and weak lensing measurements for a sample of $\sim$ 3200 $\log_{10}(M_{\star}^{\mathrm{max}}/M_{\odot}) > 11.6$ super massive galaxies. Using weak lensing, we reveal a tight connection between the stellar mass distribution of super massive central galaxies and their total dark matter halo mass. At fixed 'total' stellar mass ($M_{\star}^{\mathrm{max}}$), massive galaxies with more extended mass distributions tend to live in more massive dark matter haloes.' [27]

These lower central stellar densities and more extended stellar mass distributions within larger 'DM haloes' are consistent with the explanations given here, whereby, an expansion of the galaxy occurs due to the growth of

the curvilinear parts of the gravitational field - and, thereby, also of its form space - manifesting in isotropically stretched curvilinear geodesics with unchanging velocities yielding more extended stellar distributions with lower stellar mass densities and greater apparent dynamic masses.

5.3.6 Gravitational lensing and apparent dynamic mass

In gravitational lensing, the angle of deflection of the radiation is directly proportional to the mass of a body, or virialized agglomeration of bodies, associated with the lensing and inversely proportional to the distance of separation. So, the angle of deflection progressively diminishes with increasing separation from the body, or the agglomeration. Therefore, with evidence of curvilinear optics at significant distances from luminous bodies, then it was inferred that there exist matter fields in the vicinities of, and extending far beyond, the visible bodies. The assumed matter fields were not visible nor interacting, excepting gravitationally and, thereby, hypothesized to be DM haloes.

Currently, gravitational lensing is a technique of great utility used to determine the locations and extents of regions of curvilinear gravity that are termed DM haloes [28].

Equation (2), with $\mathrm{d}s = 0$, yields:

$$\gamma = \left[-\frac{g_{tt}}{g_{rr}}\right]^{\frac{1}{2}} = \frac{1}{a}\left(1 - \frac{r_s}{r}\right) \tag{100}$$

Where,

$$\gamma = \frac{v}{\mathrm{c}} = \frac{1}{c}\frac{\mathrm{d}r}{\mathrm{d}t} = \frac{\mathrm{d}r}{\mathrm{d}x^4} \tag{101}$$

is the speed of light scaled in units of c and $\mathrm{d}r$ is the infinitesimal coordinate radial interval traversed. The last term of eq. (100) applies in the cases of spherically symmetric bodies and agglomerations in the gpRW spacetime and is obtained by means of substitutions from eqs. (51) and (53).

For bending in the x^1x^2-plane, Huyghens' principle is applied in the form [2]:

$$\frac{\mathrm{d}\phi}{\mathrm{d}x^2} = \frac{\partial\gamma}{\partial x^1} \tag{102}$$

Where, $\mathrm{d}\phi$ is the infinitesimal angle of deflection of light. This relation shows that without changing speed, there is no change of direction. (It may be recovered from Snell's law applied in the case of corresponding infinitesimal changes of speed and direction.)

Equation (100) shows that, if the components of the metric do not vary with location, then the speed does not and, therefore, by virtue of eq. (102), the direction also does not and no lensing occurs. However, if these components *inherently* are curvilinear functions of the radius, then both speed and direction change smoothly resulting in curvilinear null geodesics; lensing. Inherent curvilinearity of metric components implies the existence of a gravitational field. [2] So, the curvilinear trajectory of light, embedded in curvilinear parts of the gravitational field in the vicinities of bodies, complements light's rectilinear trajectory embedded in flat parts of the gravitational field deep in voids.

Consider a beam of light passing near an isolated star or a virialized agglomeration of bodies. In both cases, the centroids are the origins of the coordinate frames here applied. The beam approaches the structure at a distance of r (that, in the case of a body, is greater than $2r_s$). The angle of deflection, for $a = 1$, is given by the lensing relation [2]:

$$\Delta\phi = \frac{4\mathrm{G}M}{r\mathrm{c}^2} \tag{103}$$

Where, M is the mass of the gravitationally collapsed matter within the radius r.

In the Hubble flow, the separation r increases, so - as in the case of time-like geodesics - applying the inverse time transformation to the radius as it increases in the isotropic gravitational-spatial expansion yields:

$$\Delta\phi = \frac{4\mathrm{G}Ma}{\mathrm{c}^2 r} \qquad : r = a(\chi - 2r_s) + 2r_s > 2r_s \tag{104}$$

So, the angle of deflection $\Delta\phi$, at a comoving location, remains unchanged. This process is illustrated in fig. 4 that shows, for successive constant scale factor cross-sections, the radial profiles of the deflection angle around a body, or a gravitationally bound agglomeration of bodies, of mass M. The radius, at which a fixed value of the angle of deflection occurs, smoothly increases in the Hubble expansion. So, for example, as illustrated in fig. 4, the angle of deflection, $\Delta\phi = 0.2$ radian, occurs in successive constant scale factor cross-sections. at progressively increasing radii.

Without consideration of such a gravitational-spatial expansion and its effects, this outcome may be taken as being due to the presence of a composition of matter with an apparent total dynamic mass, within the spherical region of radius r, of $M_{dyn} = Ma$, as is implied by eq. (104). This apparent dynamic mass, being greater than that of the baryonic matter $M_{bar} = M$, may then be assumed to include invisible and 'collisionless' nonbaryonic DM, amidst and extending beyond the visible matter, constituting an apparent halo mass fraction of $(a-1)/a$. So, over time, as a increases from unity, the apparent DM fraction, starting from zero, increases, eventually dominating the apparent dynamic mass distribution.

So, the growing gravitational field gives rise to isotropic stretching of the geodesics of bodies (widening orbits of constant circular speeds) and light (trajectories with increasing angles of deflections around widening lenses) in galactic neighbourhoods. This may account for the increasing apparent dynamic mass attributed to DM. Such an evolution of the apparent dynamic mass is further explored in the next subsection.

5.4 Evolution of the apparent stellar halo mass relation

Durkalec *et al.* infer that:

'Since dark matter halos grow in time... the growth in stellar mass must drop dramatically over a sustained period of time in order to follow a change in $M_\star/M_h$ by roughly an order of magnitude in [stellar mass-halo mass] SMHM, or, alternatively, the dark matter accretion rate $\langle \dot{M}_{\mathrm{H}} \rangle$ must rise precipitously, or a combination of the two.' [29]

In a similar vein, Behroozi *et al.* report:

'While the stellar mass-halo mass relation does not evolve significantly from $z = 0$ to $z = 5$, a significant evolution does occur at higher redshifts... with present data...' [30]

Consider a galaxy with a constant stellar mass $M_\star = M$, (due to negligible gas fraction and accretion and, so, with quenched star formation). Due to the expansion of the curvilinear gravitational field in the region of the galaxy, the apparent DM halo mass is given by $M'_h = M(a-1)$ and the *apparent* stellar-to-halo mass relation (aSHMR), then, is $M_\star/M'_h = 1/(a-1)$. The evolution of the aSHMR of the galaxy is followed by an observer receding, in the Hubble flow, from the galaxy over an interval corresponding to $z = 1$, when $a = 2$, to $z = 7$, when $a = 8$. (Here, the cosmic expansion rate will be taken as a proxy of the effective mean rate of expansion of the galaxy of which it is a lower limit as intragalactic regions are overdense.) Subsequently described in a frame of reference obtained by the transformation $z' = 7 - z$, observations would have commenced when the observer was at $z' = 6$, when $M'_h = M_\star$. Afterwards, the gravitational-spatial expansion, corresponding to observations obtained over an interval $z' = 6$ to $z' = 5$, caused the decline of $M_\star/M'_h$ from 1 to 0.5 due to the expansion leading to an increase of M'_h that doubled it. Subsequently, the expansion, over the interval from $z' = 5$ to $z' = 0$, caused a further decline of $M_\star/M'_h$ from 0.5 to ~ 0.14 as M'_h increased to $7M$. This process is illustrated in fig. 5.

This demonstration appears to roughly repeat, for an individual galaxy, the average apparent dynamic mass assembly - subsequent to significant accretion of baryons - of large numbers of galaxies, scattered over great distances and time, as inferred in [29] and [30] and references therein. This implies a correspondence of the evolution of the apparent halo mass assembly of an individual galaxy to the evolution, on average, of the apparent mass assembly of large numbers of galaxies observed at various redshifts. In consideration of such correspondence, Behroozi *et al.* state in [30]:

'If galaxy mass is tightly correlated with halo mass on average, it is natural to expect that individual galaxy assembly could be correlated to halo assembly.'

So, these expanding regions of gravitational lensing, as well as, the flattened and rising rotation curves and subsequent deductions of invisible clustering matter are, here, explained by the expansion of regions of curvilinear gravity extending well beyond the stellar haloes.

5.5 Geodesics and gravitational energy density

If the circular speeds of satellites and the angles of deflection of light expressed, for quasi-Schwarzschild gravitational systems, in eqs. (96) and (104), respectively, are determined by the local energy density of gravity, as may be suggested by the common dependence on the comoving radius in these equations and in the expression of the conserved gravitational energy density given in eq. (97), then the retention, in comoving locations, of the values of these geodesic characteristics may be placed on a local physical basis.

To this end, substitute $l = 1/(1 - r_s/r\,)$ into eq. (61) of the energy density around a spherically symmetric body at $a = 1$ and rewrite as:

$$l^2 - 2l + \hat{t}_t^t/\hat{t}_{t,max}^t = 0 \tag{105}$$

Where, $\hat{t}_{t,max}^t = H^2/2\kappa$ is the maximum gravitational energy density. The equation above has two solutions given as: $l = 1 \pm \sqrt{(1 - \hat{t}_t^t/\hat{t}_{t,max}^t)}$. Substitutions in eq. (88) of the circular speed at $a = 1$ show that, of the two, only

$$l = \left(1 - \frac{r_s}{r}\right)^{-1} = 1 + \sqrt{1 - \hat{t}_t^t/\hat{t}_{t,max}^t} \qquad : \ \hat{t}_t^t > 0, r > 2r_s \tag{106}$$

is physically admissible. Substituting from this equation into (88) yields:

$$v_{rot} = \frac{\mathrm{c}}{\sqrt{2}}\left[1 - \left(1 + \sqrt{1 - \hat{t}_t^t/\hat{t}_{t,max}^t}\right)^{-1}\right]^{1/2} \qquad : \ \hat{t}_t^t > 0 \tag{107}$$

Substituting from eq. (106) into the Newtonian acceleration term in eq. (86) yields the magnitude of the radial acceleration a_r as:

$$a_r = \frac{\mathrm{d}^2 r}{\mathrm{d}\tau^2} = -\frac{\mathrm{c}^2}{2r_s}\left[1 - \left(1 + \sqrt{1 - \hat{t}_t^t/\hat{t}_{t,max}^t}\right)^{-1}\right]^2 \qquad : \ \hat{t}_t^t > 0 \tag{108}$$

With regards to the orientation of the acceleration, firstly consider the case of a particle freely falling in the isotropic gravitational field around a spherically-symmetric central gravitating body. Here, the radial acceleration of the particle is normal to the spherical isopycnic surface - centred at the gravitating body's centroid that is the origin of the frame applied - that passes through it. Such surfaces satisfy the condition; $\nabla \hat{t}_t^t = 0$. So, the acceleration of the particle is collinear with the two antiparallel surface normals of the isopycnic surface, at its location, given by $\nabla^2 \hat{t}_t^t$. Since the acceleration is oriented along pathways, in the centrally-symmetric field, of locally maximal rates of decline of the energy densities, then its direction is that of the surface normal $\boldsymbol{n}$ that yields a normal derivative of the energy density satisfying the condition; $\partial \hat{t}_t^t/\partial \boldsymbol{n} < 0$.

These relations enable the *local* determination of the gravitational acceleration in the isotropic field of the spherical body. However, since the gravitational field acts purely locally in guiding peculiar motions, then, *in general*, the gravitational acceleration it induces may be determined, in these ways, from the local distribution of the field in the vicinity of the satellite.

Substituting from eq. (106) into eq. (103) yields:

$$\Delta\phi = 2\left[1 - \left(1 + \sqrt{1 - \hat{t}_t^t/\hat{t}_{t,max}^t}\right)^{-1}\right] \qquad : \ \hat{t}_t^t > 0 \tag{109}$$

Furthermore, for $a = 1$, the speed of light, given in eq. (100), may be expressed as:

$$\gamma = \left(1 + \sqrt{1 - \hat{t}_t^t / \hat{t}_{t,max}^t}\right)^{-1} \qquad : \ \hat{t}_t^t > 0 \tag{110}$$

So, the equations above describe characteristics of curvilinear time-like and null geodesics in regions of curvilinear gravity around a body in terms of the gravitational energy density.

Now, by setting $\hat{t}_t^t / \hat{t}_{t,max}^t = 1$, as it is deep in cosmic voids and in the homogeneous FLRW universe, in eqs. (107), (108), (109) and (110) then, locally, there results $v_{rot} = 0$, $a_r = 0$, $\Delta\phi = 0$, and $\gamma = 1$, respectively, as may be otherwise expected. So, these equations hold even in the gravitationally flat cosmic voids beyond the gravitationally curvilinear regions and, so, may hold everywhere.

Therefore, these equations may express the local physical dependence of geodesics - both null and time-like - on the conserved energy density of gravity. The gravitational-spatial expansion is also, in part, due to the local conservation of gravitational energy density. So, along with eqs. (50) and (97), describing the evolution of the gravitational manifold - its expansion and energy density, respectively - they may provide a physical basis for a *general* explanation of the expanding curvilinear and rectilinear geodesics that occur in the vicinities of bodies and more remotely from other quasi-Schwarzschild systems, respectively.

Expressions of geodesic quantities as functions of the gravitational energy density are, in principle, always possible for various systems that are characterized by their potentials. A dependence of geodesics on gravitational energy density would be an affirmation of the purely local influence, on bodies and radiation, expected of a physical gravitational field, as opposed to the non-local 'instantaneous action at a distance' implied by the use of the Newtonian potential.

6.0 Tidal interactions of stellar systems

Gravitational curvilinearity occurs everywhere that gravitational energy densities satisfy $0 < \hat{t}_t^t / \hat{t}_{t,max}^t < 1$. Curvilinear parts of the gravitational field - here, also referred to as *gravitational haloes* - associated with gravitating bodies and gravitationally bound agglomerations, have effective extents that are dependent on the masses of gravitationally bound matter that they enclose and on their expansions over time. For as remotely observed, these structures converge, dynamically, to quasi-Schwarzschild point mass objects [cf. §5.1]. Hence, the spherical shapes of 'DM haloes' irrespective of the morphology of the virialized baryonic distributions with which they share centroids and enclose. So, more apparently dynamically massive structures have larger gravitational haloes.

In a large halo of an apparently dynamically massive galaxy, a stellar system of lesser apparent dynamic mass - such as a dwarf galaxy, or star cluster - and, therefore, with a smaller gravitational halo is a captive if its speed is less than the escape velocity of the apparently greater dynamically massive structure. If the captive system has an *ex situ* origin, then, separately gravitationally bound before capture, both structures had gravitational energy density profiles that independently increase - with distances from their centroids - from being relatively small near their bodies, to asymptotically approaching their maximum $\hat{t}_{t,max}^t$, remotely. [Cf. Panels (a) of figs. 1 and 2.]

After capture, the apparently lesser dynamically massive stellar system exists within the gravitational halo of the larger structure as a satellite. This results in the combination of the haloes of the two structures, with overall extents in accord with the conservation of volume, the latter as the gravitational field, being divergence-free, is also incompressible. Therefore, the apparent dynamic mass of the combination is $\Sigma_i M_i a_i$, with $i = 1, 2$ (cf. §5.3.5). However, in the combination, the apparently more dynamically massive galaxy, that may be of lesser baryonic mass, becomes the progenitor as, by virtue of its larger gravitational halo, it engulfs the smaller halo and so secures the central role as the host galaxy. Over time, both *in situ* and *ex situ* baryons, the latter likely cumulatively becoming of greater baryonic mass, contribute, in these differing ways, to the formation of the gravitational halo. [30]

So, on one hand, all the gravitationally collapsed matter in the halo contributes to its apparent dynamic mass:

'The SHMR is the relation between halo mass and central galaxy mass. Whereas the SHMR has an exponentially rising slope and large scatter at the high mass end, ...' 'In observations, the total K_s-band luminosity or stellar mass in galaxy groups and clusters ... show tight relation with halo mass...' [27].

On the other hand, for example, the ongoing merger of two galactic clusters IE0657-558 [31], also known as the Bullet cluster, presents a striking demonstration of the central position and centralizing role of progenitors in mass assembly and gravitational halo formation. In the collision of the two galactic clusters parts of their hot plasma are retarded due to ram pressure. This results in the greater portion of the baryonic masses of both clusters, comprising hot plasma, being between the separating stellar components of the two clusters subsequent to their cores passing through each other.

In fig. 1 of [31] equipotential contours of the convergence of the interacting clusters, obtained by weak lensing reconstruction, are illustrated. The equipotential contours of the convergence, due to the latter being a projection of Newton's potential on the plane of the lens, coincide with isopycnic contours of the energy density of the gravitational field.

This may be obtained, here, by considering the gravitational field of a cluster described by an Hernquist model. Equations (63) and (99), along with $\hat{t}^t_{t,max} = H^2/\kappa$, yield:

$$\hat{t}^t_t/\hat{t}^t_{t,max} = \frac{1}{1+2\Phi/c^2} + \frac{2\Phi^2(\sigma_G^2/\Phi+1)}{c^2\sigma_G^2(1+2\Phi/c^2)^2} \tag{111}$$

This equation shows that gravitational equipotentials trace gravitationally isopycnic contours of a cluster with a given value of σ_G. So, close to clusters, their characteristic velocities and, so, their scale lengths, also, shape their fields, as the above equation and (63) show. These influences are discernible in the energy density profiles of the Hernquist model illustrated in fig. 2. Note the 'cored' approach to the centre, barely discernible before the expansion, it becomes more apparent in it. However, eq. (63) implies that as $r/a_G \to \infty$, then, $(\sigma_G^2/\Phi + 1) \to \sigma_G^2/\Phi$ and $\Phi \to -GM_G/r$, the latter as $\sigma_G = \sqrt{GM_G/a_G}$. In eq. (111), this yields:

$$\hat{t}^t_t/\hat{t}^t_{t,max} = \frac{1+4\Phi/c^2}{(1+2\Phi/c^2)^2} \tag{112}$$

A similar relation may also be obtained from eq. (106), with $r_s/r = -2\Phi/c^2$, for $0 \geq \Phi = -GM/r > -c^2/4$. This shows that, remotely observed, an isolated cluster gravitationally appears as a gravitating point mass object. So, undisturbed, clusters have expanding spherical gravitational haloes. This further demonstrates the quasi-Schwarzschild gravitational nature of expanding Hernquist galaxies first encountered in §5.3.5.

The fact that, for each cluster of IE0657-558, the central symmetries of the gravitational halo and the stellar mass distribution survive the collision is consistent with a robust organizing role of stellar progenitors both in stellar mass assembly and gravitational halo formation.

The absence of haloes - centrally symmetric with the two centres of X-ray brightness used in measuring the mass of the plasma - enclosing the massive plasma clouds between the clusters is taken, by the authors of [31], as being an absence of DM in those regions. However, here, this implies that the hot plasma has not collapsed gravitationally and, therefore, is not necessarily enclosed within gravitational haloes [cf. §5.1].

These outcomes attest to the *coupling* of the gravitational haloes and gravitationally collapsed matter centred on stellar progenitors.

The authors of [31] infer, from the potential, a matter distribution that follows from their appearances in Poisson's equation. The apparent dynamic masses within each of the two haloes enclosing the clusters are much greater than those of the associated baryonic fractions and the presence of the hypothesized DM is assumed by the authors. Here, expanding curvilinear parts of the gravitational field coupled to gravitationally collapsed matter offer an alternative explanation.

The energy density of a gravitational halo monotonically increases with separation from the centroid. So, the free fall of the satellite and its gravitational halo - the latter, here, called the *gravitational subhalo* - occurs within the gravitational halo of the more apparently dynamically massive central galaxy - the *host halo* - at progressively lower densities of the latter. In order to avoid discontinuities in the changing distributions of the gravitational energy of the curvilinear fields, it is proposed, here, that as the satellite falls towards the vicinity of the central galaxy, so moving from regions of higher gravitational energy densities to those of lower energy densities of the host halo, the gravitationally denser outer parts of the subhalo *accrete* to parts of the host halo of corresponding densities. So, the

gravitational subhalo, in its fall, progressively becomes more *truncated* at reducing gravitational densities in its outer parts.

Furthermore, since the energy density of the host halo reduces along with the distance from the centre, then the densities of the outer parts of the subhalo nearer to the galactic centre would be lower than those further away and, therefore, these parts would be more deeply stripped. So, an initially spherical subhalo would become misshapen, more flattened on the side closer to the centroid of the host halo and peaking on the opposite side. This stripping of the gravitational subhalo at progressively reducing densities, in favour of the host halo, also occurs under the constraint of the conservation of volume.

If the subhalo is being significantly stripped, baryons, due to being *embedded* in the outer parts of the subhalo, will also be transferred to the host halo. Equation (107) implies that the transfer of baryons from the outer parts of a subhalo to gravitationally isopycnic bordering parts of the host halo occurs as *inertial* geodesic transfers without change of circular speeds. So, at this tidal interface, stars, dust and gas change orbits from around the satellite's centroid to orbits around, or towards, the centroid of the central galaxy.

As the accelerations of stripped baryons change directions from pointing towards the centroid of the satellite to being oriented towards that of the central galaxy, they also become of different magnitudes, as implied by eq. (108). Equations (107) and (108) and the inverse proportionality - for a common circular speed at $a = 1$ - of the radius and the radial acceleration imply that the distance r_{SH} from the centroid of the satellite to any point Q on the tidal interface may be expressed by the relation $r_{SH} = R_{GQ}M/M_G$, where, R_{GQ} is the galactocentric radius of the host halo at Q, M is the mass of the baryons of the satellite, and M_G is the mass of the baryons of the central galaxy. Denoting the galactocentric radius to the centroid of the satellite as R_{GS} and the angle between R_{GS} and r_{SH} as α, then the cosine rule applied to the triangle with vertices at Q and the two centroids, along with the preceding expression of r_{SH}, yield:

$$r_{SH} = R_{GS}\left(-\cos\alpha \pm \sqrt{M_G/M - \sin^2\alpha}\right)/(M_G/M - 1) \tag{113}$$

Of the two options presented above, discarding the unphysical one leads to:

$$r_{SH} = R_{GS}\left(\sqrt{M_G/M - \sin^2\alpha} - \cos\alpha\right)/(M_G/M - 1) \approx R_{GS}\sqrt{M/M_G}\left(1 - \sqrt{M/M_G}\cos\alpha\right) \tag{114}$$

This relation locates the tidal interface between subhalo and host halo. It is spheroidal. At the pole where $\alpha = 0$, that is, nearest to the central galaxy, the subhalo is shallowest with radius $r_{SH} = R_{GS}/\left(\sqrt{M_G/M} + 1\right)$. While, it is deepest at its furthest point from the galaxy, that is, at the antipole where $\alpha = \pi$, $r_{SH} = R_{GS}/\left(\sqrt{M_G/M} - 1\right)$. Around the 'equator', where $|\alpha| = \pi/2$, the radius is given by the geometric mean of the extremal radii as $r_{SH} = R_{GS}/\sqrt{M_G/M - 1}$.

In the last term of (114), obtained assuming $M_G/M \gg 1$, the shape of the tidal interface, to a first approximation, is described by the combination of a spherical surface and a sinusoidal half-wave radial surface variation that undercuts the hemisphere nearest to the central galaxy and overlays the hemisphere further away.

With $\sqrt{M/M_G} \ll 1$, then to this second approximation, $r_{SH} \approx R_{GS}\sqrt{M/M_G}$ which, for $R_{GS} = R_P$ - the radius of the galaxy at the satellite's perigalacticon - recalls the tidal radius r_t of a DM subhalo modelled by a singular isothermal sphere (SIS): $r_t \approx R_P(\sigma_S/\sigma_H) = R_P\sqrt{M_S/M_H}$. Where, σ is the velocity dispersion, M_S is the mass of the DM subhalo within r_t and M_H is the mass of the DM host halo, also modelled by a SIS, within R_P. [32]

(The SIS model is unphysical because its mass increases indefinitely with radius - as do other prominent DM halo models, giving rise to the need for their fiducial truncations [33] - and, furthermore, it has a central mass singularity.)

During the fall, the approximate time rate of change of the tidal radius may be obtained from eq. (114) as:

$$\dot{r}_{SH} \approx \dot{R}_{GS}\sqrt{\frac{M}{M_G}} + \frac{R_{GS}}{2}\frac{\dot{M}}{M}\sqrt{\frac{M}{M_G}} \tag{115}$$

The first term on the right describes the stripping of the subhalo due only to its fall in the host halo; $\dot{R}_{GS} < 0$. The last term of the equation above describes the transfer of embedded baryons from the gravitational subhalo to the host halo, $\dot{M} < 0$, and its influence in enhancing the stripping of the subhalo. Its appearance implies a positive feedback cycle that, in the satellite's fall, drives coupled reductions of the subhalo's radii and the mass of the satellite once it is triggered by an initial tidal transfer of baryons at $r_{SH} = R_{\text{last}}$, the radius of the outermost satellite-centric baryonic matter distribution. [34] This transfer of the outer parts of the subhalo, along with baryons that may be embedded therein, is interrupted by the satellite's passage away from its perigalacticon.

So, there is a *closed tidal surface* enclosing the satellite's gravitational system.

The radial density profiles of the Eridanus and Pal 15 globular clusters - rendered in figs. 1 and 2, respectively, of [35] - exhibit overdense matter distributions extending beyond the satellites' tidal radii r_t on all sides:

'The radial profile [of Eridanus] exhibits an excess of stars outside $r \sim 1'.82$ $(\log(r) \sim 0.26)$, which continues beyond the nominal tidal radius $r > r_t = r \sim 3'.17$ and follows a power law with an index of $\gamma = -1.64 \pm 0.16$ (azimuthally averaged).' [35]

'The radial profile of Pal 15 follows closely a King profile until the local star density has dropped to ~3% of its central value ($r \sim 3'.47$ or $\log(r) \sim 0.54$), beyond which there is a strong excess of stars that continues past the nominal tidal radius and follows a power law with an index of $\gamma = -2.09 \pm 0.09$ (azimuthally averaged).' [35]

Such distributions appear to strongly support transfers of baryons across all parts of closed tidal surfaces around satellites.

A subhalo in a closed orbit of significant eccentricity will be substantially stripped during its initial approach to its perigalacticon. Then, in the separation from its perigalacticon, it accretes bordering parts of the host halo, as described by eq. (115), up to the density at its apogalacticon. However, this recovery of the gravitational subhalo may be merely a partial reinstatement of its stripped parts similar in its extents to isopycnic parts of its initial profile established before capture and when $a = 1$. This alternation of stripping of, and accretion by, the subhalo would repeat in the closed orbit that expands, along with the host halo, in the cosmic Hubble flow.

In the expansion, r_{SH} and R_{GS} both increase according to the effective scale factors of subhalo and host halo, respectively, and are better described by comoving radial variables, as are their priors - gravitational energy densities, radial accelerations and circular speeds - rendering eqs. (114) and (115) generally applicable.

Satellites in circular orbits at comoving radii from the centroid of a galactic cluster would have their growing gravitational subhaloes continuously delimited by the growing host halo. Therefore, the subhaloes expand within the host halo. So, over time, the apparent dynamic masses of such satellite galaxies and their host increase. Several such subhaloes in a galactic cluster give rise to a 'clumpy' host halo that may be revealed as such by means of Galaxy-Galaxy Strong Lensing (GGSL).

The authors of [36] set out, in part, to 'consider whether the observed number of GGSL events are consistent with theoretical predictions within the concordance cosmological model'. They report that, 'Previous studies revealed that observed small satellite galaxies were fewer in number and were less compact than expected from simulations; here, we find the opposite for cluster substructures. GGSL events that we observe show that subhalos are more centrally concentrated than predicted by simulations i.e. there is an excess not a deficit'. [36]

Equations (97) and (104) show that, at a constant scale factor, the deflection angle monotonically increases at decreasing radii and gravitational energy densities and eq. (109) and fig. 4 show that, in the gravitational-spatial expansion, over time, the deflection angle increases at all radii. Truncations of gravitational subhaloes do not affect null geodesics that still transit through them. So, although relatively small, through deep truncations resulting from existence in low gravitational energy densities of the host halo, the subhaloes reported in [36] have sufficiently extended regions of gravitational energy densities sufficiently low so as to produce the deflections required by GGSL events.

Furthermore, here, the numbers and concentrations of subhaloes depend solely on the numbers and distributions of massive gravitating bodies and virialized agglomerations of bodies that are present as satellites for, here, gravitational haloes develop anywhere there is gravitationally collapsed matter.

In the case where the stellar systems merge, the halo of the satellite - in its fall through the host halo to the latter's central structure, that is, to the host halo's lowest gravitational density - would have become completely accreted to the host halo. So, there results a single structure with its expanding gravitational halo.

After a stellar system and its halo transit through a larger halo in an open orbit, the stellar system would have lost, to its former host halo, some of its gravitational halo due to truncation. On exit, if its halo and the baryonic material embedded in its outer regions were significantly stripped then, as kinematically determined, it would appear devoid of much of its expected apparent dynamic mass. For, although its relatively high rotation speeds close to its centre are expected, the absence, at significant radii, of satellites with such speeds may be taken as being due to the absence of, otherwise expected, invisible dynamic masses. This may be the situation in the cases of certain ultra diffuse galaxies (UDGs), including NGC 1052-DF2 [37], NGC 1052-DF4 [38] and others [39].

Conversely, net transfers of fields from subhaloes to host haloes, through mergers and/or in transits, conceivably may result in the extraordinarily high apparent dynamic mass-to-light ratios, attributed elsewhere to unusually high DM fractions, of UDGs such as the Dragonfly 44 in the Coma cluster [40] and Segue 1 [41], that may have been past recipients in such interactions.

7.0 Discussion

A crucial element in these explanations is the gravitational energy pseudo-tensors of Einstein. The pseudo-tensors, according to Einstein in [2], describe the energy components of gravity. There, it is revealed that the energy pseudo-tensors of gravity and energy tensors of baryons and radiation act together in the induction of gravity. However, beyond their common participation in the induction of gravity, in the account given here, it is shown that the energy pseudo-tensors are qualitatively different from energy tensors. This is apparent even in the process of induction: pseudo-tensors induce a steadily accelerating rate of growth of the field, with respect to distance, whereas, the actions of the energy tensors diminish in the expansion.

Furthermore, energy tensors of bodies and radiation*, from time to time*, interact *locally*. Whereas, the pseudo-tensors of gravity, considered here, *at all times* and *everywhere* interact to expand the cosmic gravitational-spatial manifold. So, the scopes of the interactions are at vastly different scales. Energy tensors interact locally, with outcomes that are independent of the frames of reference used to localize their interactions. That is, energy tensors are generally covariant. Whereas, gravitational pseudo-tensors, generally, are not localizable.

Misner *et al.* state:

'At issue is not the existence of gravitational energy, but the localizability of gravitational energy. It is not localizable. The equivalence principle forbids.'

'The over-all effect one is looking at is a global effect, not a local effect.' 'That is the lesson of the nonuniqueness of the $t^{\mu\nu}$.' [11]

The cosmic expansion is a global effect of a cosmic action. The pseudo-tensors considered here act cosmically and, thereby, have no need of general covariance.

Furthermore, gravitational pseudo-tensors cannot be localized by means of a source/field bifurcation because of the auto-inductive nature of gravity whereby the induced field is also a source that is, here, proposed to be everywhere. Embodying both source and sink, energy pseudo-tensors are generally divergenceless.

Here, pseudo-tensors appear to be simply described in frames of reference that are transported, solely, in the geodesic Hubble flow. So, pseudo-tensors - that, here, act cosmically - share a preferred frame of reference with clocks that keep cosmic time.

The assumption of the vacuum presents significant challenges to gravitational sciences. It is involved in the non-local Newtonian 'instantaneous action at a distance'. It is responsible for the disconnect, in ΛCDM, of small-scale gravitational systems from the large-scale cosmic flow [3,5,18] as:

'the Einstein-Straus model has never stopped being considered as the correct answer to the lack of influence of the cosmological expansion on local systems.' [4]

For,

'The main motivation of the Einstein-Straus model was its ability to combine cosmological expansion at large scales with no observable effects on the local physics.' [4]

However, the signature of the cosmological expansion on small-scale phenomena - extended flattened, or rising, rotation curves and unexpectedly large lenses - are apparent, but misattributed to DM. Along with reducing densities within inner regions of central galaxies, with more extended stellar distributions, of more apparently dynamically massive galaxies bearing the same total stellar mass, geodesic stretching is explained by intragalactic gravitational-spatial expansions. These regions of gravitational curvilinearity smoothly extend into surrounding -

gravitationally flat and most energetically intense - cosmic voids or smoothly become indistinct as the very large scales of cosmic homogeneity are approached. So, here, vacuoles have no place.

Here, descriptions of phenomena in the cosmic expansion are crucially facilitated by the gpRW metric. Applicable in explanations of the density fluctuations, at cosmological scales in the early universe, that lead to the gravitational collapse [16], the gpRW metric, here, provides a *single dynamic* 'fluid filled' [18] cosmic spacetime enabling descriptions of small-scale phenomena attributed to DM in galaxies and to those attributed to DE in cosmic voids and at the large scales of homogeneity. In voids, the gpRW metric shares a form with the FLRW metric that is only applicable at scales large enough that the universe appears homogeneous, with the two applications essentially differing only in the time rates of change of their scale factors. In these ways, the gpRW metric appears as being fit for cosmic applications at all scales.

To explain the observable spatial expansion, various steady-state solutions have been proposed including the continual creation of matter (*e.g.* Hoyle) and the continuous creation of the DE of the vacuum [8]. The first is challenged by the conservation of energy and the second by the 'cosmological constant problem' [42].

Recognized, here, is the continuous growth of the gravitational field through the creation, in induction, of gravitational energy throughout the gravitational manifold that possesses the form of physical space, the latter as proposed here, and so results in the Hubble spatial expansion at all scales.

This proposal does not appear as being inconsistent with the *possession*, by the *non-baryonic* gravitational field, of the following: a strong and unique coupling to space; laws of unconditional conservation of energy density; powers of energetic auto-induction; and the distinctive barotrope - characterized by an *EoS* parameter of $w = -1$ and negative pressures - required to expand physical space as *prescribed*, for the same purpose, for the cosmological constant of ΛCDM, as well as, for the false vacuum of inflation [12].

Explanations based on the dynamical field avoid assumptions of exotic sources - DM and DE - and their obstinate problematics [21,42], while providing a unitary explanation of apparently mutually exclusive sets of phenomena.

8.0 Conclusions and future work

It is found that if space is the form of a cosmic gravitational field that embeds baryons and radiation, then this field would be able to generate phenomena separately attributed to DE and DM. The following outcomes support this finding:

1. Gravity, in FLRW and gpRW spacetimes, has an *EoS* parameter $w = -1$ and negative pressures. The maximum absolute magnitude both of gravitational energy density and gravitational pressure, asymptotically attained deep in cosmic voids and everywhere in the FLRW universe, is given as $H^2/2\kappa \sim$ 1.52E-27 $0.66h^2$ kg m^{-3}.
2. The expansion of space may be driven by non-thermal isobaric dynamics of the incompressible gravitational field yielding, thereby, the Hubble-Lemaître law.
3. The recognition of the dynamical regenerative auto-induction of gravity in Einstein's theory of gravity.
4. The development of a relation between the induced growth of the gravitational field and the expansion of space that yields new expressions of the Hubble parameter - in a general form and in a form particularised for the late homogeneous universe - with both having a common gravitational term of density $2H^2/\kappa$ that acts as a gravitational 'cosmological constant' of density parameter $2/3$. The *Planck* 2018 result is moderately higher, at about the 2.5σ level, than the value obtained here.
5. The use of a single metric - the gpRW metric - that, with its expanding dynamical spacetime, is applicable at all scales across the universe:
   - providing descriptions, in small-scale inhomogeneous regions, of spherically symmetric expanding curvilinear gravitational systems.
   - in homogeneous regions, it becomes a de Sitter metric or - at very large scales - a FLRW metric, according to the absence or presence, respectively, of energy tensors and, thereby, providing descriptions of the effects of the isotropic expansion on time-like and null geodesics.
6. A unitary explanation of two sets of cosmic phenomena - elsewhere separately attributed to DE and DM - as being due to influences of the isotropically expanding gravitational-spatial manifold on embedded matter and radiation:

- the redshifting of radiation in null geodesics and the accelerating recessions of bodies in time-like geodesics, as remotely observed across vast homogeneous regions and attributed to DE, may be explained by the stretching of these geodesics in the induced isotropic gravitational-spatial expansion.
- evidence from observations of massive central galaxies - that those with the same fiducial 'total' stellar mass $M_{\star}^{\max}$, but of greater apparent dynamic masses, generally have lower stellar densities within the inner 10 kpc of more extended stellar distributions - is consistent with intragalactic expansions of the field. Intragalactic expansions lead to the coincidences of the proper isotropic accelerations and the peculiar radial orbital accelerations of bodies resulting in the retentions of the values of orbital velocities and accelerations at comoving locations, geodesics stretching, that explains phenomena ascribed to DM.
- The apparent dynamic mass of an undisturbed gravitationally bound system is the product of the mass of its baryons and the scale of the expansion of its gravitational halo.

7. Generally applicable to gravitationally bound systems, the quasi-Schwarzschild asymptotic speed relation $v^4 = \mathrm{G}M_{bar}a_r$, at $r = \sqrt{M_{bar}}/f_B$ where the acceleration $a_r = \mathrm{G}$, explains the BTFR and BFJR that disfavour DM.
8. The demonstration of a potential dependence of null and time-like geodesics on the gravitational energy density. So, in the expansion, since the conservation of gravitational energy density leads to the retention of its values at comoving locations, then the dependence of geodesics on the gravitational energy density becomes a dependence on comoving radii that explains geodesic stretching.
9. A field approach, based on these relations of gravitational energy density and geodesics, provides new explanations of tidal interactions of stellar systems. Tidal stripping, during passages to perigalacticons, occurs as isopycnic transfers of the outer parts of the fluidic field of gravitational subhaloes across spheroidal tidal interfaces to gravitational host haloes that lead to inertial transfers of baryons if these are embedded in the outer parts of these subhaloes. A similar, likely diminished, transfer of the field, but from host halo to subhalo, occurs during passage to apogalacticon.

   A general expression of the radii of subhaloes at their tidal surfaces is obtained. After approximations, this relation takes a form similar to that obtained by means of the application of a singular isothermal sphere (SIS) model of interacting DM host halo and subhalo at perigalacticon, while avoiding the SIS model's unphysical aspects.

Future work is expected to continue the field approach in explorations of gravitational phenomena. Simulations will be performed to develop descriptions of the evolution of gravitational systems of different types and in differing environments. The behaviour of the field in the vicinities of event horizons will be explored.

9.0 Declarations

9.1 Funding

Not applicable

9.2 Conflicts of interests

Not applicable

9.3 Availability of data and material

Not applicable

9.4 Code availability

Not applicable

9.5 Authors' contributions

Not applicable

FIGURES

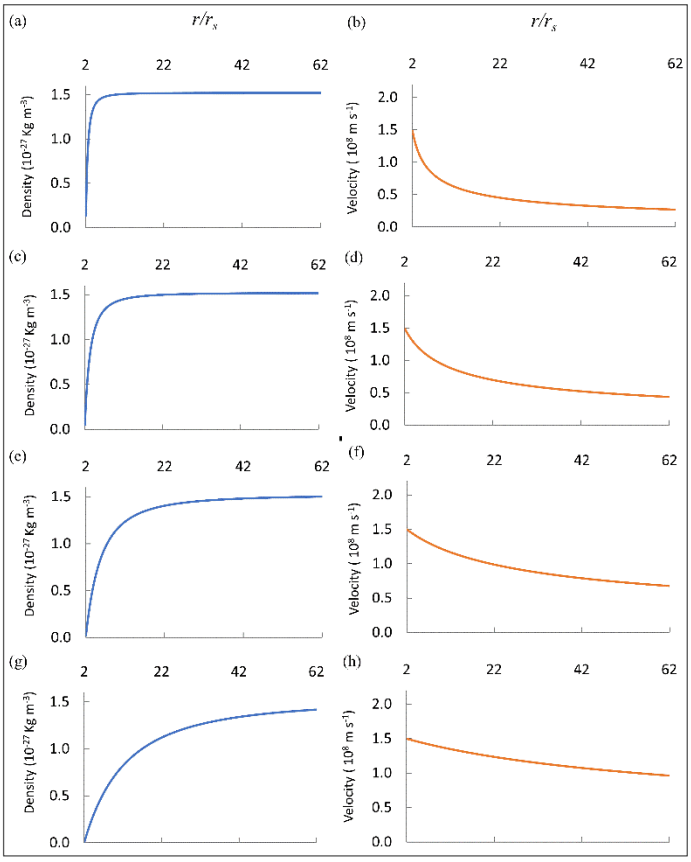

Fig. 1 Evolution of a rotation curve and gravitational energy density around a compact body

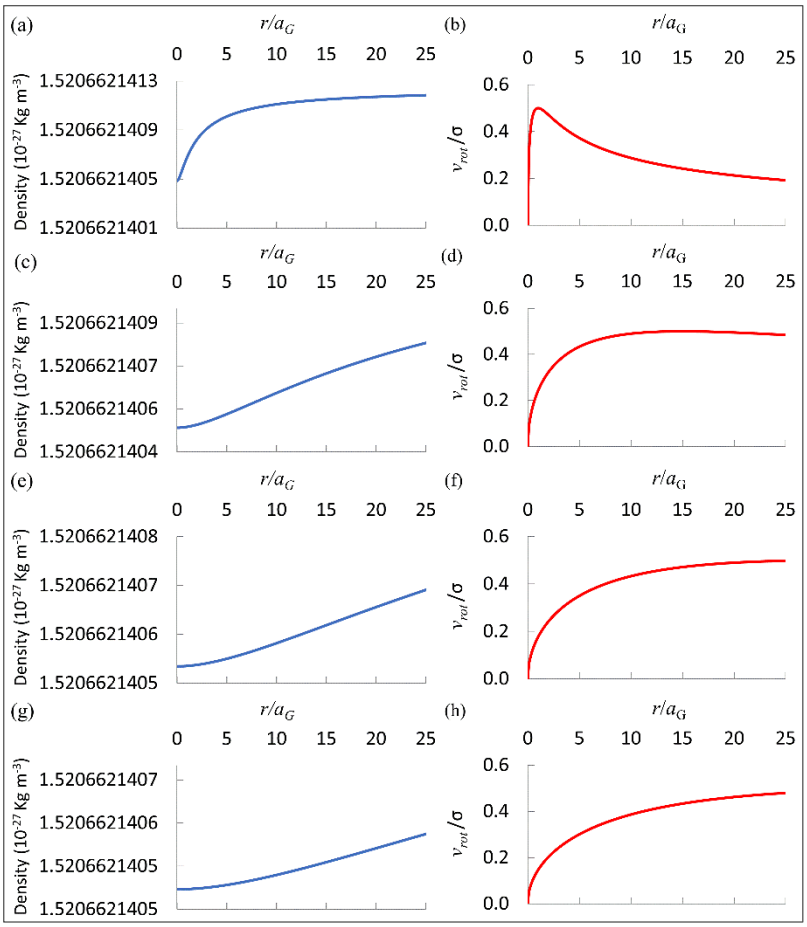

Fig. 2 Evolution of a rotation curve and gravitational energy density of spheroidal galaxy

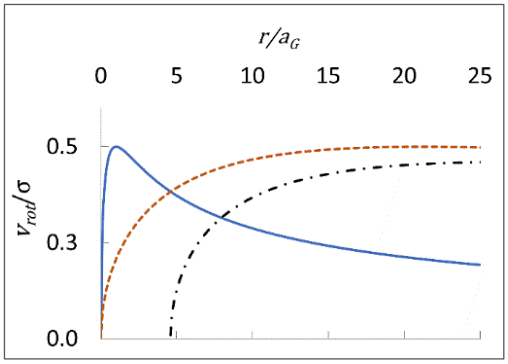

Fig. 3 Two rotation curves of a single galaxy: an earlier (solid) profile and a later (dashed) one. The dash-dot line traces the real results of differences, in quadrature, between the velocities of the earlier profile and those of the later one

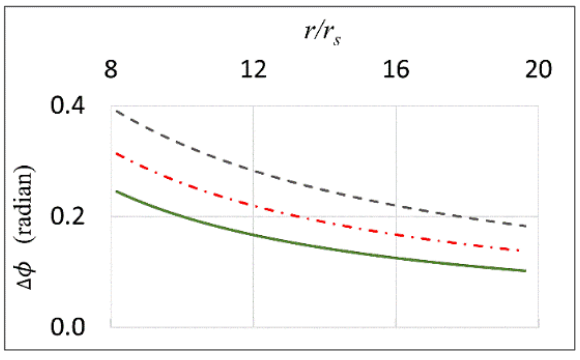

Fig. 4 Evolution of the radial profile of deflection angles. The solid curve is the earliest profile and the dashed curve is the latest one

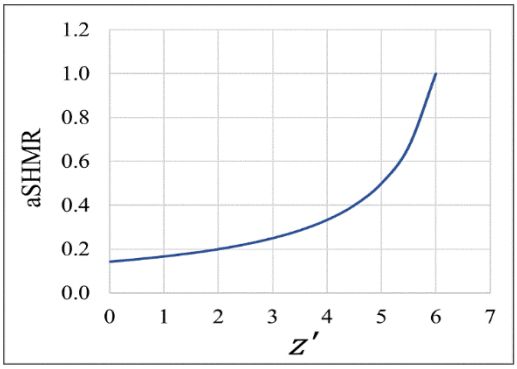

Fig. 5 Evolution of the apparent stellar-halo mass relation of a quiescent galaxy

REFERENCES

[1] A. Einstein, Sitzungsber.Preuss.Akad.Wiss.Berlin (1917) 142–152.
[2] A. Einstein, Ann. Phys. 354 (1916) 769–822.
[3] A. Einstein, E.G. Straus, Rev. Mod. Phys. 17 (1945) 120–124.
[4] M. Mars, F.C. Mena, R. Vera, Gen. Relativ. Gravit. 45 (2013) 2143–2173.
[5] R. Plaga, Astron. Astrophys. 440 (2005).
[6] J.S. Farnes, Astron. Astrophys. (2018).
[7] A. Deur, Eur. Phys. J. C (2019).
[8] A.G. Riess, A. V. Filippenko, (2001) 30–49.
[9] I.D. Karachentsev, O.G. Kashibadze, D.I. Makarov, R.B. Tully, Mon. Not. R. Astron. Soc. 393 (2009) 1265–1274.
[10] W. Hu, Ann. Phys. (N. Y). 303 (2003) 203–225.
[11] J.A. Misner, Charles W.; Thorne, Kip S.; Wheeler, Gravitation, W. H. Freeman and Company, San Francisco, 1973.
[12] A.H. Guth, Phys. Rev. D 23 (1981) 347–356.
[13] B.P. Abbott, R. Abbott, T.D. Abbott, F. Acernese, K. Ackley, C. Adams, T. Adams, P. Addesso, R.X. Adhikari, V.B. Adya, C. Affeldt, M. Afrough, B. Agarwal, M. Agathos, K. Agatsuma, N. Aggarwal, O.D. Aguiar, L. Aiello, A. Ain, P. Ajith, B. Allen, G. Allen, A. Allocca, M.A. Aloy, P.A. Altin, A. Amato, A. Ananyeva, S.B. Anderson, W.G. Anderson, S. V. Angelova, S. Antier, S. Appert, K. Arai, M.C. Araya, J.S. Areeda, N. Arnaud, K.G. Arun, S. Ascenzi, G. Ashton, M. Ast, S.M. Aston, P. Astone, D. V. Atallah, P. Aufmuth, C. Aulbert, K. AultONeal, C. Austin, A. Avila-Alvarez, S. Babak, P. Bacon, M.K.M. Bader, S. Bae, P.T. Baker, F. Baldaccini, G. Ballardin, S.W. Ballmer, S. Banagiri, J.C. Barayoga, S.E. Barclay, B.C. Barish, D. Barker, K. Barkett, F. Barone, B. Barr, L. Barsotti, M. Barsuglia, D. Barta, J. Bartlett, I. Bartos, R. Bassiri, A. Basti, J.C. Batch, M. Bawaj, J.C. Bayley, M. Bazzan, B. Bécsy, C. Beer, M. Bejger, I. Belahcene, A.S. Bell, B.K. Berger, G. Bergmann, J.J. Bero, C.P.L. Berry, D. Bersanetti, A. Bertolini, J. Betzwieser, S. Bhagwat, R. Bhandare, I.A. Bilenko, G. Billingsley, C.R. Billman, J. Birch, R. Birney, O. Birnholtz, S. Biscans, S. Biscoveanu, A. Bisht, M. Bitossi, C. Biwer, M.A. Bizouard, J.K. Blackburn, J. Blackman, C.D. Blair, D.G. Blair, R.M. Blair, S. Bloemen, O. Bock, N. Bode, M. Boer, G. Bogaert, A. Bohe, F. Bondu, E. Bonilla, R. Bonnand, B.A. Boom, R. Bork, V. Boschi, S. Bose, K. Bossie, Y. Bouffanais, A. Bozzi, C. Bradaschia, P.R. Brady, M. Branchesi, J.E. Brau, T. Briant, A. Brillet, M. Brinkmann, V. Brisson, P. Brockill, J.E. Broida, A.F. Brooks, D.A. Brown, D.D. Brown, S. Brunett, C.C. Buchanan, A. Buikema, T. Bulik, H.J. Bulten, A. Buonanno, D. Buskulic, C. Buy, R.L. Byer, M. Cabero, L. Cadonati, G. Cagnoli, C. Cahillane, J. Calderón Bustillo, T.A. Callister, E. Calloni, J.B. Camp, M. Canepa, P. Canizares, K.C. Cannon, H. Cao, J. Cao, C.D. Capano, E. Capocasa, F. Carbognani, S. Caride, M.F. Carney, J.C. Diaz, C. Casentini, S. Caudill, M. Cavaglià, F. Cavalier, R. Cavalieri, G. Cella, C.B. Cepeda, P. Cerdá-Durán, G. Cerretani, E. Cesarini, S.J. Chamberlin, M. Chan, S. Chao, P. Charlton, E. Chase, E. Chassande-Mottin, D. Chatterjee, K. Chatziioannou, B.D. Cheeseboro, H.Y. Chen, X. Chen, Y. Chen, H.-P. Cheng, H. Chia, A. Chincarini, A. Chiummo, T. Chmiel, H.S. Cho, M. Cho, J.H. Chow, N. Christensen, Q. Chu, A.J.K. Chua, S. Chua, A.K.W. Chung, S. Chung, G. Ciani, R. Ciolfi, C.E. Cirelli, A. Cirone, F. Clara, J.A. Clark, P. Clearwater, F. Cleva, C. Cocchieri, E. Coccia, P.-F. Cohadon, D. Cohen, A. Colla, C.G. Collette, L.R. Cominsky, M. Constancio Jr., L. Conti, S.J. Cooper, P. Corban, T.R. Corbitt, I. Cordero-Carrión, K.R. Corley, N. Cornish, A. Corsi, S. Cortese, C.A. Costa, M.W. Coughlin, S.B. Coughlin, J.-P. Coulon, S.T. Countryman, P. Couvares, P.B. Covas, E.E. Cowan, D.M. Coward, M.J. Cowart, D.C. Coyne, R. Coyne, J.D.E. Creighton, T.D. Creighton, J. Cripe, S.G. Crowder, T.J. Cullen, A. Cumming, L. Cunningham, E. Cuoco, T.D. Canton, G. Dálya, S.L. Danilishin, S. D'Antonio, K. Danzmann, A. Dasgupta, C.F.D.S. Costa, V. Dattilo, I. Dave, M. Davier, D. Davis, E.J. Daw, B. Day, S. De, D. DeBra, J. Degallaix, M. De Laurentis, S. Deléglise, W. Del Pozzo, N. Demos, T. Denker, T. Dent, R. De Pietri, V. Dergachev, R. De Rosa, R.T. DeRosa, C. De Rossi, R. DeSalvo, O. de Varona, J. Devenson, S. Dhurandhar, M.C. Díaz, L. Di Fiore, M. Di Giovanni, T. Di Girolamo, A. Di Lieto, S. Di Pace, I. Di Palma, F. Di Renzo, Z. Doctor, V. Dolique, F. Donovan, K.L. Dooley, S. Doravari, I. Dorrington, R. Douglas, M. Dovale Álvarez, T.P. Downes, M. Drago, C. Dreissigacker, J.C. Driggers, Z. Du, M. Ducrot, P. Dupej, S.E. Dwyer, T.B. Edo, M.C. Edwards, A. Effler,

H.-B. Eggenstein, P. Ehrens, J. Eichholz, S.S. Eikenberry, R.A. Eisenstein, R.C. Essick, D. Estevez, Z.B. Etienne, T. Etzel, M. Evans, T.M. Evans, M. Factourovich, V. Fafone, H. Fair, S. Fairhurst, X. Fan, S. Farinon, B. Farr, W.M. Farr, E.J. Fauchon-Jones, M. Favata, M. Fays, C. Fee, H. Fehrmann, J. Feicht, M.M. Fejer, A. Fernandez-Galiana, I. Ferrante, E.C. Ferreira, F. Ferrini, F. Fidecaro, D. Finstad, I. Fiori, D. Fiorucci, M. Fishbach, R.P. Fisher, M. Fitz-Axen, R. Flaminio, M. Fletcher, H. Fong, J.A. Font, P.W.F. Forsyth, S.S. Forsyth, J.-D. Fournier, S. Frasca, F. Frasconi, Z. Frei, A. Freise, R. Frey, V. Frey, E.M. Fries, P. Fritschel, V. V. Frolov, P. Fulda, M. Fyffe, H. Gabbard, B.U. Gadre, S.M. Gaebel, J.R. Gair, L. Gammaitoni, M.R. Ganija, S.G. Gaonkar, C. Garcia-Quiros, F. Garufi, B. Gateley, S. Gaudio, G. Gaur, V. Gayathri, N. Gehrels, G. Gemme, E. Genin, A. Gennai, D. George, J. George, L. Gergely, V. Germain, S. Ghonge, A. Ghosh, A. Ghosh, S. Ghosh, J.A. Giaime, K.D. Giardina, A. Giazotto, K. Gill, L. Glover, E. Goetz, R. Goetz, S. Gomes, B. Goncharov, G. González, J.M.G. Castro, A. Gopakumar, M.L. Gorodetsky, S.E. Gossan, M. Gosselin, R. Gouaty, A. Grado, C. Graef, M. Granata, A. Grant, S. Gras, C. Gray, G. Greco, A.C. Green, E.M. Gretarsson, P. Groot, H. Grote, S. Grunewald, P. Gruning, G.M. Guidi, X. Guo, A. Gupta, M.K. Gupta, K.E. Gushwa, E.K. Gustafson, R. Gustafson, O. Halim, B.R. Hall, E.D. Hall, E.Z. Hamilton, G. Hammond, M. Haney, M.M. Hanke, J. Hanks, C. Hanna, M.D. Hannam, O.A. Hannuksela, J. Hanson, T. Hardwick, J. Harms, G.M. Harry, I.W. Harry, M.J. Hart, C.-J. Haster, K. Haughian, J. Healy, A. Heidmann, M.C. Heintze, H. Heitmann, P. Hello, G. Hemming, M. Hendry, I.S. Heng, J. Hennig, A.W. Heptonstall, M. Heurs, S. Hild, T. Hinderer, D. Hoak, D. Hofman, K. Holt, D.E. Holz, P. Hopkins, C. Horst, J. Hough, E.A. Houston, E.J. Howell, A. Hreibi, Y.M. Hu, E.A. Huerta, D. Huet, B. Hughey, S. Husa, S.H. Huttner, T. Huynh-Dinh, N. Indik, R. Inta, G. Intini, H.N. Isa, J.-M. Isac, M. Isi, B.R. Iyer, K. Izumi, T. Jacqmin, K. Jani, P. Jaranowski, S. Jawahar, F. Jiménez-Forteza, W.W. Johnson, N.K. Johnson-McDaniel, D.I. Jones, R. Jones, R.J.G. Jonker, L. Ju, J. Junker, C. V. Kalaghatgi, V. Kalogera, B. Kamai, S. Kandhasamy, G. Kang, J.B. Kanner, S.J. Kapadia, S. Karki, K.S. Karvinen, M. Kasprzack, W. Kastaun, M. Katolik, E. Katsavounidis, W. Katzman, S. Kaufer, K. Kawabe, F. Kéfélian, D. Keitel, A.J. Kemball, R. Kennedy, C. Kent, J.S. Key, F.Y. Khalili, I. Khan, S. Khan, Z. Khan, E.A. Khazanov, N. Kijbunchoo, C. Kim, J.C. Kim, K. Kim, W. Kim, W.S. Kim, Y.-M. Kim, S.J. Kimbrell, E.J. King, P.J. King, M. Kinley-Hanlon, R. Kirchhoff, J.S. Kissel, L. Kleybolte, S. Klimenko, T.D. Knowles, P. Koch, S.M. Koehlenbeck, S. Koley, V. Kondrashov, A. Kontos, M. Korobko, W.Z. Korth, I. Kowalska, D.B. Kozak, C. Krämer, V. Kringel, B. Krishnan, A. Królak, G. Kuehn, P. Kumar, R. Kumar, S. Kumar, L. Kuo, A. Kutynia, S. Kwang, B.D. Lackey, K.H. Lai, M. Landry, R.N. Lang, J. Lange, B. Lantz, R.K. Lanza, A. Lartaux-Vollard, P.D. Lasky, M. Laxen, A. Lazzarini, C. Lazzaro, P. Leaci, S. Leavey, C.H. Lee, H.K. Lee, H.M. Lee, H.W. Lee, K. Lee, J. Lehmann, A. Lenon, M. Leonardi, N. Leroy, N. Letendre, Y. Levin, T.G.F. Li, S.D. Linker, T.B. Littenberg, J. Liu, R.K.L. Lo, N.A. Lockerbie, L.T. London, J.E. Lord, M. Lorenzini, V. Loriette, M. Lormand, G. Losurdo, J.D. Lough, C.O. Lousto, G. Lovelace, H. Lück, D. Lumaca, A.P. Lundgren, R. Lynch, Y. Ma, R. Macas, S. Macfoy, B. Machenschalk, M. MacInnis, D.M. Macleod, I. Magaña Hernandez, F. Magaña-Sandoval, L. Magaña Zertuche, R.M. Magee, E. Majorana, I. Maksimovic, N. Man, V. Mandic, V. Mangano, G.L. Mansell, M. Manske, M. Mantovani, F. Marchesoni, F. Marion, S. Márka, Z. Márka, C. Markakis, A.S. Markosyan, A. Markowitz, E. Maros, A. Marquina, F. Martelli, L. Martellini, I.W. Martin, R.M. Martin, D. V. Martynov, K. Mason, E. Massera, A. Masserot, T.J. Massinger, M. Masso-Reid, S. Mastrogiovanni, A. Matas, F. Matichard, L. Matone, N. Mavalvala, N. Mazumder, R. McCarthy, D.E. McClelland, S. McCormick, L. McCuller, S.C. McGuire, G. McIntyre, J. McIver, D.J. McManus, L. McNeill, T. McRae, S.T. McWilliams, D. Meacher, G.D. Meadors, M. Mehmet, J. Meidam, E. Mejuto-Villa, A. Melatos, G. Mendell, R.A. Mercer, E.L. Merilh, M. Merzougui, S. Meshkov, C. Messenger, C. Messick, R. Metzdorff, P.M. Meyers, H. Miao, C. Michel, H. Middleton, E.E. Mikhailov, L. Milano, A.L. Miller, B.B. Miller, J. Miller, M. Millhouse, M.C. Milovich-Goff, O. Minazzoli, Y. Minenkov, J. Ming, C. Mishra, S. Mitra, V.P. Mitrofanov, G. Mitselmakher, R. Mittleman, D. Moffa, A. Moggi, K. Mogushi, M. Mohan, S.R.P. Mohapatra, M. Montani, C.J. Moore, D. Moraru, G. Moreno, S.R. Morriss, B. Mours, C.M. Mow-Lowry, G. Mueller, A.W. Muir, A. Mukherjee, D. Mukherjee, S. Mukherjee, N. Mukund, A. Mullavey, J. Munch, E.A. Muñiz, M. Muratore, P.G. Murray, K. Napier, I. Nardecchia, L. Naticchioni, R.K. Nayak, J. Neilson, G. Nelemans, T.J.N. Nelson, M. Nery, A. Neunzert, L. Nevin, J.M. Newport, G. Newton, K.K.Y. Ng, T.T. Nguyen, D. Nichols, A.B. Nielsen, S. Nissanke, A. Nitz, A. Noack, F. Nocera, D. Nolting, C. North, L.K. Nuttall, J. Oberling, G.D. O'Dea, G.H. Ogin, J.J. Oh, S.H. Oh, F. Ohme, M.A. Okada, M.

Oliver, P. Oppermann, R.J. Oram, B. O'Reilly, R. Ormiston, L.F. Ortega, R. O'Shaughnessy, S. Ossokine, D.J. Ottaway, H. Overmier, B.J. Owen, A.E. Pace, J. Page, M.A. Page, A. Pai, S.A. Pai, J.R. Palamos, O. Palashov, C. Palomba, A. Pal-Singh, H. Pan, H.-W. Pan, B. Pang, P.T.H. Pang, C. Pankow, F. Pannarale, B.C. Pant, F. Paoletti, A. Paoli, M.A. Papa, A. Parida, W. Parker, D. Pascucci, A. Pasqualetti, R. Passaquieti, D. Passuello, M. Patil, B. Patricelli, B.L. Pearlstone, M. Pedraza, R. Pedurand, L. Pekowsky, A. Pele, S. Penn, C.J. Perez, A. Perreca, L.M. Perri, H.P. Pfeiffer, M. Phelps, O.J. Piccinni, M. Pichot, F. Piergiovanni, V. Pierro, G. Pillant, L. Pinard, I.M. Pinto, M. Pirello, M. Pitkin, M. Poe, R. Poggiani, P. Popolizio, E.K. Porter, A. Post, J. Powell, J. Prasad, J.W.W. Pratt, G. Pratten, V. Predoi, T. Prestegard, M. Prijatelj, M. Principe, S. Privitera, G.A. Prodi, L.G. Prokhorov, O. Puncken, M. Punturo, P. Puppo, M. Pürrer, H. Qi, V. Quetschke, E.A. Quintero, R. Quitzow-James, F.J. Raab, D.S. Rabeling, H. Radkins, P. Raffai, S. Raja, C. Rajan, B. Rajbhandari, M. Rakhmanov, K.E. Ramirez, A. Ramos-Buades, P. Rapagnani, V. Raymond, M. Razzano, J. Read, T. Regimbau, L. Rei, S. Reid, D.H. Reitze, W. Ren, S.D. Reyes, F. Ricci, P.M. Ricker, S. Rieger, K. Riles, M. Rizzo, N.A. Robertson, R. Robie, F. Robinet, A. Rocchi, L. Rolland, J.G. Rollins, V.J. Roma, R. Romano, C.L. Romel, J.H. Romie, D. Rosińska, M.P. Ross, S. Rowan, A. Rüdiger, P. Ruggi, G. Rutins, K. Ryan, S. Sachdev, T. Sadecki, L. Sadeghian, M. Sakellariadou, L. Salconi, M. Saleem, F. Salemi, A. Samajdar, L. Sammut, L.M. Sampson, E.J. Sanchez, L.E. Sanchez, N. Sanchis-Gual, V. Sandberg, J.R. Sanders, B. Sassolas, B.S. Sathyaprakash, P.R. Saulson, O. Sauter, R.L. Savage, A. Sawadsky, P. Schale, M. Scheel, J. Scheuer, J. Schmidt, P. Schmidt, R. Schnabel, R.M.S. Schofield, A. Schönbeck, E. Schreiber, D. Schuette, B.W. Schulte, B.F. Schutz, S.G. Schwalbe, J. Scott, S.M. Scott, E. Seidel, D. Sellers, A.S. Sengupta, D. Sentenac, V. Sequino, A. Sergeev, D.A. Shaddock, T.J. Shaffer, A.A. Shah, M.S. Shahriar, M.B. Shaner, L. Shao, B. Shapiro, P. Shawhan, A. Sheperd, D.H. Shoemaker, D.M. Shoemaker, K. Siellez, X. Siemens, M. Sieniawska, D. Sigg, A.D. Silva, L.P. Singer, A. Singh, A. Singhal, A.M. Sintes, B.J.J. Slagmolen, B. Smith, J.R. Smith, R.J.E. Smith, S. Somala, E.J. Son, J.A. Sonnenberg, B. Sorazu, F. Sorrentino, T. Souradeep, A.P. Spencer, A.K. Srivastava, K. Staats, A. Staley, M. Steinke, J. Steinlechner, S. Steinlechner, D. Steinmeyer, S.P. Stevenson, R. Stone, D.J. Stops, K.A. Strain, G. Stratta, S.E. Strigin, A. Strunk, R. Sturani, A.L. Stuver, T.Z. Summerscales, L. Sun, S. Sunil, J. Suresh, P.J. Sutton, B.L. Swinkels, M.J. Szczepańczyk, M. Tacca, S.C. Tait, C. Talbot, D. Talukder, D.B. Tanner, M. Tápai, A. Taracchini, J.D. Tasson, J.A. Taylor, R. Taylor, S. V. Tewari, T. Theeg, F. Thies, E.G. Thomas, M. Thomas, P. Thomas, K.A. Thorne, K.S. Thorne, E. Thrane, S. Tiwari, V. Tiwari, K. V. Tokmakov, K. Toland, M. Tonelli, Z. Tornasi, A. Torres-Forné, C.I. Torrie, D. Töyrä, F. Travasso, G. Traylor, J. Trinastic, M.C. Tringali, L. Trozzo, K.W. Tsang, M. Tse, R. Tso, L. Tsukada, D. Tsuna, D. Tuyenbayev, K. Ueno, D. Ugolini, C.S. Unnikrishnan, A.L. Urban, S.A. Usman, H. Vahlbruch, G. Vajente, G. Valdes, N. van Bakel, M. van Beuzekom, J.F.J. van den Brand, C. Van Den Broeck, D.C. Vander-Hyde, L. van der Schaaf, J.V. van Heijningen, A.A. van Veggel, M. Vardaro, V. Varma, S. Vass, M. Vasúth, A. Vecchio, G. Vedovato, J. Veitch, P.J. Veitch, K. Venkateswara, G. Venugopalan, D. Verkindt, F. Vetrano, A. Viceré, A.D. Viets, S. Vinciguerra, D.J. Vine, J.-Y. Vinet, S. Vitale, T. Vo, H. Vocca, C. Vorvick, S.P. Vyatchanin, A.R. Wade, L.E. Wade, M. Wade, R. Walet, M. Walker, L. Wallace, S. Walsh, G. Wang, H. Wang, J.Z. Wang, W.H. Wang, Y.F. Wang, R.L. Ward, J. Warner, M. Was, J. Watchi, B. Weaver, L.-W. Wei, M. Weinert, A.J. Weinstein, R. Weiss, L. Wen, E.K. Wessel, P. Weßels, J. Westerweck, T. Westphal, K. Wette, J.T. Whelan, S.E. Whitcomb, B.F. Whiting, C. Whittle, D. Wilken, D. Williams, R.D. Williams, A.R. Williamson, J.L. Willis, B. Willke, M.H. Wimmer, W. Winkler, C.C. Wipf, H. Wittel, G. Woan, J. Woehler, J. Wofford, K.W.K. Wong, J. Worden, J.L. Wright, D.S. Wu, D.M. Wysocki, S. Xiao, H. Yamamoto, C.C. Yancey, L. Yang, M.J. Yap, M. Yazback, H. Yu, H. Yu, M. Yvert, A. Zadrożny, M. Zanolin, T. Zelenova, J.-P. Zendri, M. Zevin, L. Zhang, M. Zhang, T. Zhang, Y.-H. Zhang, C. Zhao, M. Zhou, Z. Zhou, S.J. Zhu, X.J. Zhu, A.B. Zimmerman, M.E. Zucker, J. Zweizig, E. Burns, P. Veres, D. Kocevski, J. Racusin, A. Goldstein, V. Connaughton, M.S. Briggs, L. Blackburn, R. Hamburg, C.M. Hui, A. von Kienlin, J. McEnery, R.D. Preece, C.A. Wilson-Hodge, E. Bissaldi, W.H. Cleveland, M.H. Gibby, M.M. Giles, R.M. Kippen, S. McBreen, C.A. Meegan, W.S. Paciesas, S. Poolakkil, O.J. Roberts, M. Stanbro, V. Savchenko, C. Ferrigno, E. Kuulkers, A. Bazzano, E. Bozzo, S. Brandt, J. Chenevez, T.J.-L. Courvoisier, R. Diehl, A. Domingo, L. Hanlon, E. Jourdain, P. Laurent, F. Lebrun, A. Lutovinov, S. Mereghetti, L. Natalucci, J. Rodi, J.-P. Roques, R. Sunyaev, P. Ubertini, Astrophys. J. 848 (2017) L13.

[14] E. Harrison, Astrophys. J. 403 (1993) 28.

[15] Astron. Astrophys. (2020).
[16] E. Bertschinger, Phys. D Nonlinear Phenom. 77 (1994) 354–379.
[17] L.M. Widrow, J. Dubinski, Astrophys. J. 631 (2005) 838–855.
[18] G.F.R. Ellis, R. Goswami, Gen. Relativ. Gravit. 45 (2013) 2123–2142.
[19] R. Van De Weygaert, Proc. Int. Astron. Union 11 (2014) 497–523.
[20] V.C. Rubin, Proc. Natl. Acad. Sci. U. S. A. 90 (1993) 4814–4821.
[21] D.H. Weinberg, J.S. Bullock, F. Governato, R.K. De Naray, A.H.G. Peter, Proc. Natl. Acad. Sci. U. S. A. 112 (2015) 12249–12255.
[22] R. Genzel, N.M.F. Schreiber, H. Übler, P. Lang, T. Naab, R. Bender, L.J. Tacconi, E. Wisnioski, S. Wuyts, T. Alexander, A. Beifiori, S. Belli, G. Brammer, A. Burkert, C.M. Carollo, J. Chan, R. Davies, M. Fossati, A. Galametz, S. Genel, O. Gerhard, D. Lutz, J.T. Mendel, I. Momcheva, E.J. Nelson, A. Renzini, R. Saglia, A. Sternberg, S. Tacchella, K. Tadaki, D. Wilman, Nature 543 (2017) 397–401.
[23] S.S. McGaugh, J.M. Schombert, G.D. Bothun, W.J.G. de Blok, Astrophys. J. 533 (2000) L99–L102.
[24] S. McGaugh, Galaxies 8 (2020) 25–28.
[25] D. Edmonds, D. Minic, T. Takeuchi, Int. J. Mod. Phys. D 29 (2020).
[26] M. Mosleh, S. Tacchella, A. Renzini, C. Marcella Carollo, A. Molaeinezhad, M. Onodera, H.G. Khosroshahi, S. Lilly, ArXiv (2017).
[27] S. Huang, A. Leauthaud, A. Hearin, P. Behroozi, C. Bradshaw, F. Ardila, J. Speagle, A. Tenneti, K. Bundy, J. Greene, C. Sifón, N. Bahcall, Mon. Not. R. Astron. Soc. 492 (2020) 3685–3707.
[28] M. Montes, I. Trujillo, Mon. Not. R. Astron. Soc. 482 (2019) 2838–2851.
[29] A. Durkalec, O. Le Fèvre, S. De La Torre, A. Pollo, P. Cassata, B. Garilli, V. Le Brun, B.C. Lemaux, D. MacCagni, L. Pentericci, L.A.M. Tasca, R. Thomas, E. Vanzella, G. Zamorani, E. Zucca, R. Amorín, S. Bardelli, L.P. Cassarà, M. Castellano, A. Cimatti, O. Cucciati, A. Fontana, M. Giavalisco, A. Grazian, N.P. Hathi, O. Ilbert, S. Paltani, B. Ribeiro, D. Schaerer, M. Scodeggio, V. Sommariva, M. Talia, L. Tresse, D. Vergani, P. Capak, S. Charlot, T. Contini, J.G. Cuby, J. Dunlop, S. Fotopoulou, A. Koekemoer, C. López-Sanjuan, Y. Mellier, J. Pforr, M. Salvato, N. Scoville, Y. Taniguchi, P.W. Wang, Astron. Astrophys. 576 (2015).
[30] P. Behroozi, R.H. Wechsler, A.P. Hearin, C. Conroy, Mon. Not. R. Astron. Soc. 488 (2019) 3143–3194.
[31] D. Clowe, M. Bradač, A.H. Gonzalez, M. Markevitch, S.W. Randall, C. Jones, D. Zaritsky, Astrophys. J. (2006).
[32] O.Y. Gnedin, Astrophys. J. (2003).
[33] R.H. Wechsler, J.L. Tinker, Annu. Rev. Astron. Astrophys. (2018).
[34] D.E. McLaughlin, R.P. van der Marel, Astrophys. J. Suppl. Ser. 161 (2005) 304–360.
[35] G.C. Myeong, H. Jerjen, D. Mackey, G.S. Da Costa, Astrophys. J. 840 (2017) L25.
[36] M. Meneghetti, G. Davoli, P. Bergamini, P. Rosati, P. Natarajan, C. Giocoli, G.B. Caminha, R.B. Metcalf, E. Rasia, S. Borgani, F. Calura, C. Grillo, A. Mercurio, E. Vanzella, Science (80-.). (2020).
[37] P. Van Dokkum, S. Danieli, Y. Cohen, A. Merritt, A.J. Romanowsky, R. Abraham, J. Brodie, C. Conroy, D. Lokhorst, L. Mowla, E. O'Sullivan, J. Zhang, Nature 555 (2018) 629–632.
[38] P. van Dokkum, S. Danieli, R. Abraham, C. Conroy, A.J. Romanowsky, Astrophys. J. 874 (2019) L5.
[39] Q. Guo, H. Hu, Z. Zheng, S. Liao, W. Du, S. Mao, L. Jiang, J. Wang, Y. Peng, L. Gao, J. Wang, H. Wu, Nat. Astron. 4 (2020) 246–251.
[40] P. van Dokkum, A. Wasserman, S. Danieli, R. Abraham, J. Brodie, C. Conroy, D.A. Forbes, C. Martin, M. Matuszewski, A.J. Romanowsky, A. Villaume, Astrophys. J. 880 (2019) 91.
[41] A. Frebel, J.D. Simon, E.N. Kirby, Astrophys. J. 786 (2014).
[42] D. Huterer, D.L. Shafer, Reports Prog. Phys. (2018).